Contents

Accelerator Physics, Technologies, and Facilities

Donald L. Hartill

Cornell University, Ithaca, NY 14853

Stephen D. Holmes

Fermi National Accelerator Laboratory, Batavia, IL 60510

Robert B. Palmer

Brookhaven National Laboratory, Upton, NY 11973

Ronald D. Ruth

Stanford Linear Accelerator Center, Stanford, CA 94309

Working Group Members

R. Brinkman,	*DESY*
A. Chao,	*Stanford Linear Accelerator Center*
B. Danly,	*Massachusetts Institute of Technology*
G. Dugan,	*Cornell University*
M. Harrison,	*Brookhaven National Laboratory*
M. Holtkamp,	*DESY*
G. Jackson,	*Fermi National Accelerator Laboratory*
T. Katsouleas,	*University of Southern California*
D. Neufer,	*CEBAF*
N. Phinney,	*Stanford Linear Accelerator Center*
A. Sessler,	*Lawrence Berkeley Laboratory*
R. Siemann,	*Stanford Linear Accelerator Center*
K. Takata,	*KEK*
P. Tenenbaum,	*SLAC and UC Santa Cruz*
M. Tigner,	*Cornell University*
T. Weiland,	*TH–Darmstadt*
I. Wilson,	*CERN*

1 Introduction

Since the invention of the cyclotron in the early 1930's, the particle accelerator and storage ring have been the instruments of choice for scientists engaged in particle physics research. Historic advances in high-energy and particle physics have been, and are expected to continue to be, dependent upon advances in accelerator facilities and the underlying technologies upon which they are based. Over the past sixty years these technologies have provided nearly a million-fold increase in beam energy, accompanied by facilities whose size is measured in kilometers rather than meters, and whose costs are now measured in hundreds of millions, or even billions, of dollars.

Accelerators in operation today generally fall into two classes: hadron accelerators and electron accelerators. The majority of contemporary high-energy physics experiments use accelerators in which counter-circulating beams are brought into collision. This mode of operation provides the most efficient utilization of beam energy for producing high-mass particles. The highest energies are attained in hadron colliders while electron-positron colliders are used in applications in which a premium is placed upon having all available energy carried by the interacting constituents.

The highest energy accelerator facility in the world today is the Tevatron at Fermilab. This facility, the first high-energy accelerator ever constructed utilizing superconducting magnets, provides proton-antiproton collisions at 1.8 TeV in the center-of-mass, with a luminosity currently exceeding 1×10^{31} cm^{-2} s^{-1}. The Tevatron collider is the only currently operational hadron collider in the world and is the only facility of any type at which the top quark can be produced and its properties measured. The construction and operation of the Tevatron made possible development of the concepts of the Superconducting Super Collider and the Large Hadron Collider (LHC).

Hadron accelerators are often operated to provide opportunities for fixed target experiments. The Alternating Gradient Synchrotron (AGS) at Brookhaven National Laboratory currently provides 30 GeV proton

and lower energy secondary beams for use in neutrino physics, searches for new particles, a measurement of the muon's anomalous magnetic moment, and searches for and studies of rare kaon decays. This accelerator is planned to serve as the injector to the new Nuclear Physics facility RHIC later in this decade. Proton beams at 800 GeV, accompanied by a variety of secondary beams, are also available at the Fermilab Tevatron for use in fixed target experiments during periods in which the collider is not running. The focus here is on deep inelastic neutrino scattering, CP violation in rare K decays, and charm spectroscopy.

Electron colliders operational in the world today come in two types and operate in two distinct energy regimes. Colliders in the lower energy regime are exclusively based on circular accelerators. These facilities include the VEPP–2M collider in Novosibirsk, Russia, the Beijing Electron Positron Collider (BEPC), the Cornell Electron Storage Ring (CESR), and the Tristan collider at KEK in Tsukuba, Japan. These facilities operate at center-of-mass energies that range between 1.0 GeV and 60 GeV. Typical operations are tuned to the resonance associated with a particular heavy quark-antiquark bound state, *e.g.*, the ϕ at VEPP-4m, the J/Ψ at BEPC, and the $\Upsilon(4S)$ at CESR. The highest luminosity attained in any of these colliders is 3×10^{32} cm^{-2} s^{-1} at the CESR facility.

Two electron collider facilities currently operate at the energy of the Z (90 GeV in the center of mass)—the Stanford Linear Collider (SLC) and the Large Electron Positron Collider (LEP) at CERN. The SLC is the first linear collider ever constructed and demonstrates the technology that is required to extend further the energy reach of electron-positron colliders. The LEP facility is a circular storage ring 27 km in circumference and most likely represents the largest circular electron accelerator that will ever be built. LEP currently operates with a luminosity in excess of 2×10^{31} cm^{-2} s^{-1} and SLC at about 5×10^{29} cm^{-2} s^{-1}.

Finally, HERA, a hybrid facility currently operational at the DESY laboratory in Hamburg, Germany, provides electron-proton collisions at approximately 300 GeV in the center-of-mass. The facility is based on an electron accelerator operating at 30 GeV and a superconducting proton accelerator operating at 820 GeV both located in a common, 6.3 km, tunnel.

Two major new facilities, and one major upgrade, are currently under construction in the United States. The Fermilab Main Injector Project will replace the existing Main Ring at Fermilab and boost luminosity in the Tevatron Collider by a factor of five, while simultaneously providing beams for a 120 GeV fixed target program. The PEP–II project at SLAC will construct an asymmetric electron-positron collider operating at the $\Upsilon(4S)$ resonance for use in CP violation studies in the B system. The luminosity goal for this facility is 3×10^{33} cm^{-2} s^{-1}. Finally, an upgrade of the existing CESR facility is aimed at providing a luminosity of 1×10^{33} cm^{-2} s^{-1}, again at the $\Upsilon(4S)$ but in a symmetric collider mode. Each of these projects is expected to be completed around 1998. World-wide facilities under construction today include an asymmetric B Factory at KEK and ϕ Factories in Frascatti, Italy (DAΦNE), and in Novosibirsk, Russia (VEPP–2M).

It currently appears likely that CERN will proceed with construction of the LHC sometime in the near future. This facility, to be located in the existing LEP-tunnel, is proposed to provide proton-proton collisions at 14 TeV in the center-of-mass with a luminosity of 1×10^{34} cm^{-2} s^{-1}. It is expected that this project will be completed in the middle of the coming decade.

Further new facilities and upgrades that could be brought to a state of reviewable proposals over the next several years include further possible luminosity (to 1×10^{33} cm^{-2} s^{-1}) and/or energy (to 4 TeV in the center-of-mass) upgrades of the Tevatron collider, and a next generation of electron-positron linear colliders. Research and development aimed at development of technologies that could support a 500 GeV linear collider, upgradable to 1500 GeV, is underway at a variety of centers world-wide.

Despite the existence of a plan for continued extension of research opportunities over the next decade, it should be recognized that the long-term future of high-energy physics requires a continuing investment in development of accelerator technologies. Technologies currently or nearly in hand are sufficient to allow exploration of physics at the TeV scale. Moving beyond, within the confines of facilities of the current physical size and cost, will require either the development of new technologies or achievement of significant cost reduction in existing technologies. It is not too early to start thinking about a hadron collider that could be built after the LHC with 4–5 times the energy reach. Cost would be a major consideration in the construction of such a facility and so any development program would have to focus on cost reduction as well as technological goals. One may also find that departures from the standard way of thinking, *e.g.*, muon or gamma colliders, represent a highly effective means of proceeding.

As seen in the Table of Contents, the results of this working group have been divided into six primary sections. Section 2 covers Hadron Facilities, from the current state of the art all the way to a possible 30×30 TeV collider. Section 3 treats Electron Linear Collider Facilities, beginning with a summary of the status of the first linear collider, the SLC, and moving on to cover various approaches and test facilities for validating the enabling technologies. Section 4 covers Electron-Positron Circular Collider Facilities. In Section 5, we look further to the

future in our review of Advanced Accelerators. Finally, in the Conclusions, we discuss several key points that have been distilled from the contributions to this report.

2 Hadron Facilities

Hadron accelerators and storage rings have provided the US HEP program with research opportunities at the high-energy frontier for nearly forty years. Following the invention of the strong focusing concept in the early 1950's a series of proton accelerators of ever increasing energy has been constructed in the United States and Europe. Included in this group are the Brookhaven Alternating Gradient Synchrotron (AGS); the Proton Synchrotron (PS), the Intersecting Storage Rings (ISR), and Super Proton Synchrotron (SPS) at CERN; the proton ring in the HERA facility at DESY; and the Main Ring and Tevatron accelerators at Fermilab. While the basic accelerator design has largely changed only in scale, advances in the underlying technology have allowed a nearly 250-fold increase in the center-of-mass energy achieved in these facilities. The advent of superconducting magnets and the invention of stochastic cooling have spurred the latest advances.

The highest energy accelerator facility in the world today is the Tevatron at Fermilab. This facility, the first high-energy accelerator ever constructed utilizing superconducting magnets, provides proton-antiproton collisions at 1.8 TeV in the center-of-mass, with a luminosity currently exceeding 1×10^{31} cm^{-2} s^{-1}. The construction and operation of the Tevatron made possible development of the concepts of the Superconducting Super Collider (SSC) and the Large Hadron Collider (LHC).

The construction of the SSC has been the highest priority construction project in the US HEP program over the preceding decade. The construction in Waxahachie, Texas of this project, a superconducting proton-proton collider operating at a center-of-mass energy of 40 TeV, was canceled by the United States government in the fall of 1993. The cancellation of the SSC has prompted a complete reexamination of future options in both the United States and abroad, most notably in Europe. It now appears likely that the construction of the LHC will proceed in Europe over the next ten or so years. This facility, when completed, will provide proton-proton collisions at 14 TeV in the center-of-mass, eclipsing the energy reach of the Fermilab Tevatron early in the next century.

This report describes a study of options for future hadron facilities in the United States and identification of the R&D programs that need to be supported if such facilities are to be realized. The material presented here was prepared at a workshop held at the Indiana University Cyclotron Facility over the period July 6–10, 1994 [1].

2.1 Current State of the Art in Hadron Colliders

The Fermilab Tevatron is the highest energy collider operational in the world today. Protons and antiprotons counter-circulate within the Tevatron superconducting accelerator, colliding in two interaction regions. Collisions at 1.8 TeV in the center-of-mass are observed by the "CDF" and "DØ" detectors. The Tevatron is currently operating with a luminosity in the range $1\text{–}1.5\times10^{31}$ cm^{-2} s^{-1}. Completion of the Fermilab Main Injector (FMI) project, currently under construction, is expected to yield a luminosity in the range $5\text{–}10\times10^{31}$ cm^{-2} s^{-1} in the year 1999. The increase in luminosity is primarily related to an increase in the antiproton production rate achievable with the newly constructed Main Injector accelerator. It is anticipated that improvements to the Tevatron refrigeration system will allow operation at 2.0 TeV in the center-of-mass during this period. However, further energy enhancements are dependent on construction of either higher field dipole magnets (presently 4.4 T), or of a larger circumference tunnel (presently 6280 m), or both. Completion of the FMI will also afford the opportunity for a 120 GeV fixed target program concurrent with collider operations at Fermilab.

The design of the SSC was based on the technology developed in the Fermilab Tevatron. Proton-proton collisions were to be produced by colliding protons counter-circulating in separate rings utilizing dipole magnets operating at 6.6 T. The total circumference was to have been 87 km. A total energy of 40 TeV in the center-of-mass with a luminosity of 1×10^{33} cm^{-2} s^{-1} was anticipated. The magnetic dipole field of 6.6 T represented a 50% improvement over the Tevatron design. This improvement was primarily derived from improved performance in superconducting cable over the period 1978–1988. The design of the magnets also showed significant advances over the Tevatron in the area of reduced heat leak through advanced cryostat design. The new significant design issues in the SSC were largely related to the enhanced level of synchrotron radiation and to the achievement of significantly smaller transverse emittances in the SSC relative to the Tevatron. The superconducting magnet design for the SSC was fully developed with technology transfer to industry underway at the time of cancellation of the project.

The LHC complex, as currently proposed, is very similar to the SSC except for the smaller scale. The design energy is 14 TeV in the center-of-mass with a luminosity of 1×10^{34} cm^{-2} s^{-1}. The LHC is proposed to be constructed in the existing, 27 km, LEP tunnel. The magnet, a two-in-one design operating at 8.7 T, represents a significant extension of the SSC design. Models of this magnet have been successfully built and tested. If this project proceeds as currently proposed it

is anticipated that operations will commence sometime around the year 2005.

2.2 Future Hadron Facilities

A workshop on "Future Hadron Facilities in the US" was held at the Indiana University Cyclotron Facility over the period July 6–10, 1994. Workshop participation included 52 registrants from 17 institutions in the United States and from CERN in Europe. This workshop was held under the auspices of the Accelerator Physics, Technologies and Facilities Working Group of the DPF Long Term Planning Study.

The specific goals of the Indiana workshop were three-fold:

- Development of a defensible parameter list for a 1×10^{33} cm^{-2} s^{-1} luminosity upgrade of the Tevatron $\bar{p}$–p collider at Fermilab, with an optional 2×2 TeV energy upgrade within the existing enclosure.
- Development of a defensible parameter list for a 1×10^{34} cm^{-2} s^{-1}, 30×30 TeV p–p collider.
- Identification of R&D requirements for achieving the stated parameters.

The two facilities examined were chosen because they were felt to span the potential needs of the US HEP community following the completion of the Main Injector upgrade at Fermilab, and through and beyond the period of utilization of the LHC in Europe. It was felt that the necessary R&D required to realize either of these facilities would likely provide a strong basis for nearly any direction that the community wished to move in the realm of hadron facilities over the next twenty years or so. The work of this meeting rests upon and extends previous studies of higher energy options in the Tevatron tunnel, as chronicled in the 1988 Snowmass Proceedings, and the extensive design and development work completed at the SSC Laboratory.

Six working groups were charged with identifying the technology issues related to each of the potential facilities. The working groups and their leaders were:

Magnets:	J. Tompkins, Fermilab
Cryogenics & Vacuum:	T. Peterson, Fermilab W. Turner, LBL
Antiproton Sources:	J. Marriner, Fermilab
Injectors:	R. York, Michigan State
Interaction Regions:	S. Peggs, Brookhaven
Lattice & Beam Dynamics:	M. Syphers, Brookhaven

These groups were assisted by two teams with overall responsibility for coordinating study and evaluating parameters for each of the two facilities mentioned above. These two teams were:

- 2×2 TeV $\bar{p}$–p collider at Fermilab:
  G. Jackson (Fermilab)
  R. Siemann (Stanford Linear Accelerator Center)
- 30×30 TeV p–p collider:
  A. Chao (Stanford Linear Accelerator Center)
  G. Dugan (SSC Laboratory)
  M. Harrison (Brookhaven National Laboratory)

The main body of this report is composed of the reports from each of the coordinating teams; reports from the working groups may be found in the workshop proceedings.

2.2.1 Design Issues

Luminosity and/or Energy Upgrades of the $\bar{p}$–p Collider at Fermilab. Design issues for an improvement program aimed at achieving a luminosity in excess of 1×10^{33} cm^{-2} s^{-1} in the Tevatron $\bar{p}$–p collider at Fermilab, as well as possibilities for creating a facility operating at 2×2 TeV within the existing enclosure were studied. Such a facility represents a factor of twenty improvement in luminosity over performance expected following the Main Injector upgrade. Performance parameters are listed in Table 1, where Tev* refers to the luminosity upgrade alone, and DiTevatron to the combined luminosity and energy upgrade. As noted in the table energy and luminosity upgrades can be considered separately with an additional factor of two in luminosity achievable through the energy upgrade.

The primary design issue for this facility is the antiproton production/accumulation rate. An accumulation rate of $9\times10^{11}\bar{p}$/hour is required to support a luminosity of 2×10^{33} cm^{-2} s^{-1}. This represents nearly a factor of twenty beyond the present performance of the Antiproton Source at Fermilab, and a factor of six beyond the performance expected in the Main Injector era. In addition a new facility is required in which up to 10^{13} antiprotons can be stored prior to injection into the collider. The current accumulation capability of the Antiproton Accumulator is about $2\text{–}3\times10^{12}$ antiprotons. Potential solutions to these issues are related to an increase in the number of protons targeted per hour and increased cooling bandwidth. At least one, and perhaps two, new rings are required. Details may be found in Section 2.3 and in Ref. 1.

Secondary design issues are related to providing the required magnetic fields and gradients, and understanding beam stability and dynamics with large numbers of bunches in each beam. The achievement of 2 TeV in the existing Tevatron tunnel requires dipole magnets operating at 8.8 T and quadrupoles in the interaction regions with gradients of 210 T/m. The dipole field required is a factor of 33% beyond that achieved in the SSC development program and is comparable to current achievements in the LHC program. The achievement of this field is not considered a major challenge. Development of the large aperture, 210 T/m, quadrupole represents a greater challenge. The development of such a magnet would probably

Table 1: Tevatron Upgrade Parameters.

Parameter	Main Injector	TeV*	DiTevatron
Beam energy (GeV)	1000	1000	2000
Peak luminosity ($cm^{-2}s^{-1}$)	8.3×10^{31}	1.0×10^{33}	2.0×10^{33}
Protons per bunch	3.3×10^{11}	2.4×10^{11}	2.4×10^{11}
Antiprotons per bunch	3.6×10^{10}	1.0×10^{11}	0.9×10^{11}
Proton emittance 95%, normalized (mm-mr)	30 π	18 π	18 π
Antiproton emittance, 95%, normalized (mm-mr)	20 π	18 π	18 π
β^* (cm)	35	25	25
Bunches/beam	36	108	108
Bunch spacing (ns)	395	132	132
Total number of protons	1.2×10^{13}	2.6×10^{13}	2.6×10^{13}
Total number of antiprotons	1.3×10^{12}	1.1×10^{13}	1.0×10^{13}
Interaction regions	2	2	2
Bunch length, rms (cm)	43	26	22
Integrated luminosity (pb^{-1}/wk)	17	200	400
Interactions per crossing at 45 m	2.2	9	17
Total antiproton tune shift (2 IR's)	0.016	0.019	0.019
Total proton tune shift	0.003	0.008	0.008
Peak antiproton loss rate at 90 mb ($\bar{p}/hr^{-1}$)	5.4×10^{10}	7.0×10^{11}	13×10^{11}
Antiproton stacking rate ($\bar{p}/hr^{-1}$)	1.5×10^{11}	1.0×10^{12}	1.0×10^{12}

closely parallel the development of the interaction region quadrupoles required for the LHC program. It should be noted that the magnet design is strongly impacted by the potential need to support a slow extracted beam program at 2 TeV. The decision of whether to include such a performance specification would have to be made fairly early in the development program

A number of potential issues relating to operations with a large number of bunches deserve further study. These include the long range beam-beam interaction, intrabeam scattering, issues related to the production and preservation of low emittance, and single beam instabilities. Many of these issues could be addressed through beam studies in the Tevatron.

Many of the beam dynamics issues referred to above could be ameliorated through reduction of the number of bunches. The motivation for operating with large numbers of bunches is reduction of the number of interactions per crossing at the detectors. For example, with a luminosity of 2×10^{33} cm^{-2} s^{-1} the number of interactions/crossing seen in the detectors ranges from 2.5 to 17 as the number of bunches is varied between 750 and 108. It is obvious that a dialog between accelerator and detector designers will have to take place early within the developmental period of such a facility in order to select the appropriate number of bunches.

For a luminosity upgrade of the Tevatron unaccompanied by an energy upgrade essentially all the above issues remain with the exception of those related to magnet development.

The 30×30 TeV p–p Collider. Design concepts for a collider operating at an energy a factor of four beyond LHC and a factor of one-and-a-half beyond the SSC were investigated. Comparison of the LHC and 30×30 TeV parameters is given in Table 2. While the energy of such a facility is only 50% higher than that planned for the SSC, it was recognized fairly quickly that the design and operational issues of such a machine would be quite different due to the enhanced role of synchrotron radiation. A proton collider operating at 30 TeV per beam, with dipole fields of 10 T or greater would represent the first hadron facility in which the role of synchrotron radiation went beyond being irrelevant, as at the Tevatron, or a nuisance, as at LHC and SSC. Radiation damping in a 30×30 TeV collider has a significant impact on the operating characteristics. Every effort must be taken to understand how best to utilize synchrotron radiation as an aid for simplifying the design of the facility.

The number one design issue in such a facility is clearly the dipole magnets. Fields of 10–15 T are required to keep the size of the ring manageable (where manageable means equal to the SSC). Quadrupoles with gradients of 250 T/m are required for the interaction regions. Achieving fields above 10 T will not be

Table 2: LHC and 30×30 TeV Parameters. Peak luminosity for the 30×30 TeV machine is achieved after several hours of storage.

Parameter	LHC	30×30 TeV
Beam energy (TeV)	7	30
Peak luminosity ($cm^{-2}s^{-1}$)	1.0×10^{34}	1.0×10^{34}
Protons per bunch	1.0×10^{11}	2.4×10^{10}
Proton emittance, 95%, normalized (mm-mr)	22.5 π	9 π
β^* (cm)	50	20
Bunches	2835	2030
Bunch length, rms (cm)	7.5	4
Arc dipole field (T)	8.7	12.5
Circumference (km)	26.7	60
Rev. frequency (kHz)	11.25	5
Synchrotron radiation power (kW/ring)	3.5	29
Linear power density (W/m)	0.2	0.6
Crossing half-angle (μrad)	0	50
Integrated luminosity (pb^{-1}/wk)	2000	2000
Bunch spacing (ns)	25	100
Interactions per crossing at 60 mb	19	60

easy. It is felt that 10 T is achievable but probably represents the maximum reach of the currently employed NbTi/cosθ technology. Going past 10 T will require new technology. It is difficult to predict at the moment a rate of development for such technologies.

Synchrotron radiation damping, with damping times of 4–5 hours, is shown to have a substantial positive impact on the performance of a 30×30 TeV collider. However, one must remove the heat generated within the cold magnets. The linear heat load for the parameters described below is three times that being planned for in the LHC. As in the case of the Tevatron upgrade there is a strong coupling between relaxing the challenges to the accelerator builders at the expense of interactions per crossing seen by the experimenters. In this case fewer bunches reduces the magnitude of the synchrotron radiation heat load problems. For the example given in Section 2.4, a luminosity of 1×10^{34} cm^{-2} s^{-1} is obtained with a bunch spacing of 100 ns accompanied by 60 interactions/crossing.

Options for staging such a facility, *e.g.*, starting out with lower energy or with a single ring and proton-antiproton collisions, were not examined in this study. In general one would expect the luminosity achievable to scale with energy as the energy is lowered (at a fixed circumference), and the proton-antiproton luminosity to be approximately a factor of ten lower than the proton-proton case.

Conclusions. Upgrading the Fermilab $\bar{p}$–p collider complex to either 1×10^{33} cm^{-2} s^{-1} at 1×1 TeV, or to 2×10^{33} cm^{-2} s^{-1} at 2×2 TeV is an aggressive goal. Increasing the antiproton production rate by a factor of 6 beyond that anticipated following completion of the Main Injector is the key. Several ideas exist for accomplishing this, but none are mature at this stage. Further design and development work are required to generate assurance of achieving this performance. Long range beam-beam effects are likely to be important if the Tevatron were configured to run with many (> 100) bunches at high ($>1\times10^{33}$) luminosity. Machine studies in the Tevatron could shed much light on this issue.

A proton-proton collider operating at 60 TeV in the center-of-mass, and with a luminosity of 1×10^{34} cm^{-2} s^{-1}, is a reasonable goal for the next hadron facility following the LHC. The possibility of utilizing synchrotron radiation emittance damping to enhance the performance, and simplify the construction, of a next generation hadron collider looks promising enough to warrant further attention. An operating energy in the range of 25–40 TeV/beam would require 12.5 ± 3 T dipoles. As in all high-energy hadron facilities, magnets are the key. A reinvigorated US superconducting magnet R&D program will be needed to support these aims. Facility cost will clearly be a significant design consideration and needs to be integrated into thinking on even the most preliminary designs. Cost minimization through simplification of injector performance specifications, utilization of existing facilities and infrastructure, optimization of fabrication and procurement strategies, and staging all deserve considerable thought.

There is a real trade off between relaxation of accelerator parameters and increasing the number of interactions per crossing in each of these facilities. There must be a close interaction between accelerator and detector designers to identify an optimum bunch spacing.

2.3 Luminosity and/or Energy Upgrades to the Tevatron $\bar{p}$–p Collider

A preliminary evaluation of a high-luminosity 2×2 TeV collider in the Tevatron tunnel was undertaken at the workshop. The parameters that were distributed at the beginning of the workshop and were the focus of much of the discussion are given in Table 3 in the "Original DiTevatron" column. The peak luminosity would be $L \sim 2\times10^{33}$ cm^{-2} s^{-1} achieved with 750 bunches spaced 19 ns apart. There would be 2.5 interactions per crossing in

Table 3: Tevatron Upgrade Workshop Parameters.

Parameter	1994 Actual	Main Injector	DiTevatron Original	DiTevatron Modified
Beam energy (GeV)	900	1000	2000	2000
Peak luminosity ($\times 10^{30}$ cm^{-2} s^{-1})	12.0	123	1980	1980
Protons/bunch ($\times 10^{9}$)	185	380	60	238
$\bar{p}$s/bunch	50	36	16.5	90
Proton emittance (95%,πmm-mrad)	22	30	5	18
$\bar{p}$ emittance (95%,π mm-mrad)	14	15	5	18
β^* (cm)	35	25	25	25
Bunches/beam	6	36	750	108
Bunch spacing (ns)	3493	395	18.9	132
Total protons ($\times 10^{12}$)	1.11	13.7	45.0	25.7
Total $\bar{p}$s ($\times 10^{12}$)	0.30	1.30	12.38	9.8
Interaction regions	2	2	2	2
Fract momentum spread ($\times 10^{-4}$)	6.0	5.0	0.9	2.4
rms bunch length (cm)	55	45	8	22
Crossing half angle (mr)	0	0	0.12	0
Luminosity form factor due to hourglass and crossing angle	0.62	0.58	0.69	0.79
Integrated luminosity (pb^{-1}/wk, 33% duty factor)	2.4	25	400	400
Interactions/crossing (45 mb)	1.9	3.2	2.5	17
Total $\bar{p}$ tune shift (2 IRs)	0.012	0.020	0.019	0.019
Total proton tune shift	0.005	0.004	0.005	0.005
Peak$\bar{p}$ loss rate (10^{10}/hr, 90 mb)	0.78	8.0	130	130
Stacking rate (10^{10}/hr)	4.5	15	100	100

the particle physics detectors assuming a 45 mb cross section. As discussed below some of the problems with the original parameters identified during the workshop could be solved by reducing the number of bunches at the cost of increasing the interactions per crossing to 17. These are given in the "Modified DiTevatron" column. The parameters for the current (1994) Tevatron run and the first run planned with the Main Injector are given in the table for comparison.

The major elements of either upgrade are additional accelerator(s) to increase substantially the antiproton production rate and, for the energy upgrade, a new superconducting ring replacing the existing Tevatron.

Implementation. *Lattice:* A crossing angle of 120 μrad is used to separate the beams at the interaction regions. After that, electrostatic separators are needed to establish spiral orbits in the arcs to avoid other unwanted conditions. These separators must be placed where the appropriate β-function is large and points are needed with 90° phase advance between horizontal and vertical. A lattice needs to be developed that satisfies these criteria with a footprint consistent with the Tevatron tunnel, possibly with minor modifications.

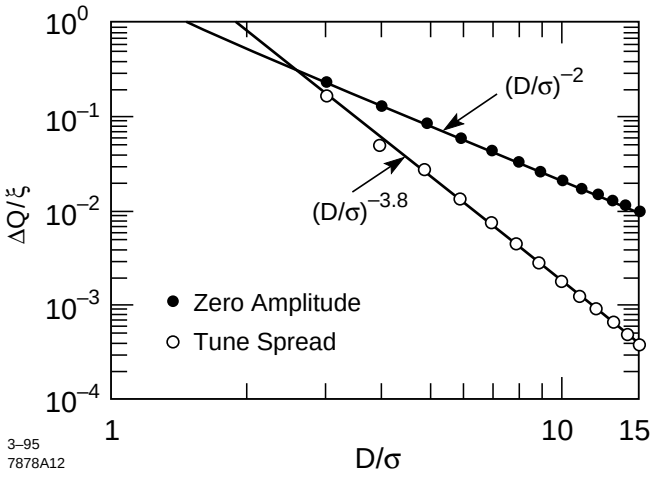

Figure 1: Parasitic beam-beam interaction. The tune shift of a zero amplitude particle and the tune spread for particles with $2\,\sigma$ amplitudes of oscillation. These are normalized to the head-on beam-beam tune shift. D is the center-to-center separation and σ is the rms beam size.

Beam Intensity: There are 1500 parasitic collisions. The tune shift of a zero amplitude particle and the tune spread for particles with oscillation amplitudes up to 2σ are plotted in Fig. 1. These are normalized to the head-on tune-shift, and the approximation has been made that the beams are round at the parasitic crossing point. Bunches are separated by $D/\sigma = 4$–5 in present Tevatron operation where there are ten parasitic collisions and no significant problems observed from

them. Keeping the same ratio of parasitic to head-on tune spread, the separation should become $D/\sigma \sim 15$–20. Since the emittance and energy spread are smaller in the DiTevatron, the beam size is smaller, and roughly the same center-to-center separation as used at present should be adequate for this consideration.

The average tune shift is more of a problem because there are a number of effects that cannot be compensated by changing the lattice tune. These include the difference in proton and $\bar{p}$ tunes, approximately $0.014\sigma^2/D^2$ per parasitic collision, and rapidly changing tunes during injection of the opposing beam. A theoretical analysis is needed, and the effects of parasitic collisions should be studied experimentally by looking at the behavior of an antiproton bunch in the presence of a fixed target proton beam.

The average proton current is comparable to the beam used in fixed target operation. Coupled bunch instabilities have been observed there, and they have been cured by tuning of cavity higher-mode frequencies. In addition, reducing the higher mode Q's could be used as a cure also, and the average current does not present a problem.

The single bunch longitudinal and transverse instability limits have been estimated, and the longitudinal microwave instability sets the impedance limit. The high-frequency impedance limit is $Z/n \leq 2\Omega$ which is be compared with the estimated Tevatron impedance, $Z/n \approx 5\Omega$. The new collider ring will have to have a lower impedance, and the microwave instability seems to be a performance limit for upgrades that do not replace the Tevatron. Of course, this can be studied experimentally.

The emittance growth rate due to intrabeam scattering has been estimated in two ways. A two hour horizontal emittance growth time was calculated by scaling from the SSC [2], and a growth time an order of magnitude longer was found using approximations in the original Piwinski reference [3]. If the first result was correct, intrabeam scattering would dominate the luminosity lifetime and it would be unacceptably short. The disagreement between the calculations is due to strong dependence on lattice functions which are not known, and a better calculation must be performed when they are.

Magnets: The 8.8 T dipole magnet technology that is needed for the DiTevatron remains to be proved, but this should be done soon as part of LHC development. The good field aperture may have to be comparable to that of the present Tevatron, 7.5-cm diam., to allow adequate separation at parasitic crossing points. SSC magnets could be run at low temperature to test the feasibility of those magnets for producing 8.8 T, but they do not have sufficient good field aperture. A design iteration addressing field quality had been planned as part of SSC development.

A gradient of 150 T/m, as required for the lattice quadrupoles, is comparable to the present Fermilab IR quad gradient of 140 T/m and the SSC lattice quadrupole gradient of 220 T/m. Scaling of present Tevatron lattice would require IR quadrupole gradients of 280 T/m. This is not feasible, but this is not a problem since the design $\beta^* = 25$ cm has been reached in lattice designs with a lower gradient of 210 T/m. Accommodating the electrostatic separators is a more serious issue.

Vacuum: The critical energy for a 2 TeV proton beam in an 8.8 T magnetic field is 3.8 eV which is close to the work function of many metals. Desorption rates have not been measured for these energies, so the impact on the vacuum system is not clear.

Low Emittance Proton Source: The present performance of the Fermilab Booster is that it accelerates batches of 84 bunches with a single bunch intensity of 4×10^{10} and longitudinal and transverse emittances of 0.08 eV-s and 10 π mm-mrad, respectively. The intensity must be higher and the transverse emittance lower for the DiTevatron, and the space charge tune shift in the Booster would be a factor of 2–3 times higher. This cannot be achieved with the present linac, and the linac energy would have to be raised to roughly 0.8–1 GeV to avoid emittance degradation from space charge. The space charge tune shift at injection to the Main Injector is low, and that should not present a problem.

Modifications to the Fermilab ion source and low energy beam optics are needed for the low transverse emittance. The requirements are within the ranges of developments for the SSC.

Antiproton Production: The $\bar{p}$ stacking rate is 5×10^{10}/hour at the present time, and this must be increased to 10^{12}/hour for high luminosity. The consensus of the antiproton source group was that at least two additional accelerators for manipulating the $\bar{p}$ phase space, cooling and accumulating $\bar{p}$'s would be required [4]. Common features of the sources considered are:

- stochastic cooling in the present Accumulator ring;
- followed by additional stacking in a new, high-energy accumulator ring;
- $\bar{p}$ recovery from the previous collider store which gives some flexibility in store length; and
- an 8–16 GHz cooling system.

The differences between approaches were:

- the role of the present Debuncher ring in a new $\bar{p}$ source,
- whether one or six 84-bunch Booster batches of Main Injector beam were targeted,
- proton beam manipulations before targeting,
- targeting, and
- antiproton manipulations after targeting.

The different approaches are detailed in the report from the antiproton source group. All of them have advantages and drawbacks, and none is developed sufficiently to judge feasibility, reliability, and cost. The viability of a high-luminosity collider in the Tevatron tunnel depends on developing an adequate $\bar{p}$ source, and the research and development associated with that is crucial.

Number of Bunches: The original parameters had 750 bunches to get a small number of interactions per crossing. With a limit on $\bar{p}$ production, the transverse emittance must be small for high luminosity and the longitudinal emittance must be small for the short bunch needed for crossing at an angle. These considerations lead to a high proton phase space density and the dominant problems of the original parameter list: space charge tune shift at injection into the Booster and intrabeam scattering (which needs to be checked as discussed above).

The modified parameters are for 108 bunches. Longitudinal coalescing could be used, as it is now, to reduce the space charge tune shift in the Booster, and the larger emittances make intrabeam scattering unimportant.

The situation with parasitic beam-beam collisions does not change substantially. While the number of parasitic collisions is reduced by a factor of 7, the beam sizes are larger, and the required separation could be larger although D/σ is smaller.

Conclusions. This workshop was helpful for identifying potential problems and suggesting areas of research. The most important ones are:

- Antiproton production is the key to high luminosity in the Tevatron. No fatal flaws were found in the approaches considered, but because of their preliminary nature, the trade-offs, costs, and potential impact on the Main Injector fixed target program, they need to be evaluated carefully.
- Parasitic beam-beam interactions would produce substantial tune shifts and tune spreads because of the large number of bunches in either case. The parasitic beam-beam interaction needs to be studied theoretically and experimentally to evaluate the impact. The required separation will determine the required good field aperture and magnet costs.
- The two DiTevatron parameter lists are contrasted by the number of interactions per crossing and phase space density of the proton beam. If the intrabeam scattering lifetime is as short as calculated by scaling from the SSC, the original list is flawed. If that is not the case, a linac energy increase and modifications to the low energy portion of the linac would be required for the phase space density in the original list. The modified list does not have these accelerator physics problems, but does have 17 interactions per crossing, which needs to be considered by experimenters.

Finally, a comparison of the DiTevatron parameters with the actual current performance shows that a 2×2 TeV high-luminosity collider in the Tevatron tunnel would represent a substantial extension. Fortunately, experiments are possible to test many aspects of the design, clarify the issues we have raised, and provide an opportunity to see unexpected ones. A concerted experimental effort would be a wise investment.

2.4 A High-Luminosity 30×30 TeV Proton Collider

This section summarizes the basic conceptual ideas that were developed during the workshop. Using 30 TeV as an example we looked at the potential consequences of a hadron collider where synchrotron radiation was sufficient to produce significant emittance damping. The machine footprint was "SSC–like" and consisted of two interaction regions and two arc sections. The desired luminosity regime was $\sim 10^{34}\,\mathrm{cm}^{-2}\,\mathrm{s}^{-1}$ in a proton-proton, 2-in-1 magnet environment. No detailed parameter adjustment was made to achieve any exact performance goals however, interest was focused more on the consequences of parametric variations.

Optimizations. Synchrotron radiation, broadly speaking, produces two main issues. Emittance damping which results in enhanced beam phase space density and is a positive attribute, and radiated power into the bore tube producing vacuum and cooling complications. The conceptual goal of this study involved utilizing the former while mitigating the latter in what we perceive to be a reasonable fashion.

The synchrotron radiation damping rate is determined by the collision energy and the dipole field, thus for a fixed set of these parameters the factor linking the damping rate to the radiated power is the number of circulating protons in the machine. Minimizing the circulating current for a fixed luminosity argues for lower beta-star at the IP and increased bunch spacing/intensities. The maximum luminosity for a fixed circulating current is obtained by increasing the bunch intensity and bunch spacing. This can be accomplished by a bunch coalescing in the injector chain. The practical limits to this exercise are determined by the experimental consequences of the increased number of events per bunch crossing. Another issue which becomes important for low beam currents, is particle burn-off at the IRs. Significant particle burn-off results in short luminosity lifetimes which pushes the machine operation in the direction of short store lengths. This in turn requires a relatively rapid cycling injector.

On the positive side, significant emittance damping provides luminosity enhancement and may also result in less sensitivity to emittance growth arising from the beam-beam interaction, *i.e.*, increase the tolerable tune

shift limit. Insensitivity to many of the traditional sources of emittance growth in hadron colliders can be expected to result in slackening of tolerances in many areas and thus a simpler, cheaper and more robust machine. Integrated luminosity is not strongly correlated to the initial beam size which simplifies the injector complex. Since significant emittance growth can be accepted during the injection cycle, field quality requirements on the arc magnets (invariably defined by low energy criteria) can be relaxed. Likewise, less sensitivity to persistent and eddy current phenomena, can be used to increase the dynamic range of the machine energy to simplify the injector specifications. Similarly, beam transfer issues are less complicated with a lack of stringent emittance growth requirements. Matching, kicker specifications and damping systems will all benefit. Instrumentation is helped by (relatively speaking) large beam sizes at injection and significant photon emission at high energies. Emittance growth due to vibration effects and power supply noise in the arcs will be ameliorated by the emittance damping, maintaining beam collisions must still be assured however. Reduced circulating beam currents also result in less stored energy in the beams, which, while still a very difficult issue, is less of a challenge than might have been expected from a straightforward scaling of LHC/SSC parameters.

Parameters. A partial parameter list for a 30×30 TeV machine is shown in Table 4. The column labeled "Original" represents the starting point for the study; "Modified" represents the developed set described here. The collision energy of 30 TeV was chosen purely to illustrate the potential consequences of operating a hadron machine in a radiation damping regime. It should be emphasized that there is an energy window where this behavior applies and is correlated to the assumed dipole field. If the machine energy is too low then the damping is insufficient to be useful. If the energy is too high then the radiated power becomes prohibitive for the cryogenic magnets. The injection energy is defined by the somewhat arbitrary choice of collision energy together with a choice of 30:1 for the dynamic range which seems reasonable with an allowance for 50% emittance growth at flat bottom. The dipole field of 12.5 T was chosen as a representation of next generation superconducting magnets though, as we demonstrate, a range of dipole fields can be accommodated in this approach. A marginal parameter remix can produce similar machine characteristics with lower dipole fields as can non-FODO lattices. The desired injector beam emittance of 1 π mm-mrad rms was taken from the SSC injector chain specifications somewhat arbitrarily. As alluded to in the next section, the luminosity evolution is relatively insensitive to initial emittance values. The criteria for injected beam parameters would appear to be set by the somewhat less demanding requirement that beam should stay in the machine for the $\sim$ 30 minute filling time rather than any emittance specifications. Since this is difficult to quantify in the short time period of a workshop we chose the SSC-like parameters. The 20 cm beta-star was picked to be the lowest value that the IR working group deemed realistic. The rf parameters were picked to deliver a bunch length consistent with the beta-star value.

The total beam current was loosely defined by the desire to produce an $\sim$ 8 hour optimum store length. The bunch intensity, bunch spacing, and hence number of bunches, was influenced by stability considerations and the projected 90 events per bunch crossing at maximum luminosity. It would appear that the LHC with 16 events per crossing has removed the option of event by event vertex reconstruction from the detectors. We have pushed this harder. Since this is one of the more controversial aspects of this design we expect further discussion on this point. Every cloud is reputed to have a silver lining, and the increased beam granularity does provide much more time between crossings for trigger processing than the LHC, for example.

The initial beam-beam tune shift is relatively benign but does increase during the store. We assumed a tolerable tune shift limit of $\sim$ 0.03 which is a modest increase on the 0.02–0.025 achieved today.

A crucial parameter in this conceptual exercise is the radiated beam power per unit length. We chose a value of 0.6 W/m which is approximately a threefold increase over the LHC. At this level a bore tube liner is necessary but vacuum issues arising from the desorbed gases are certainly tractable as are cryogenic problems associated with the heat removal. As discussed in the vacuum/cryogenic section of this workshop report power densities as high as 3 W/m could be handled with increased complexity in the various systems and beam conditioning scenarios. Since there is almost a straight trade-off between events per crossing and radiated power, and the situation with respect to either issue is complicated we imagine further discussions on this point.

The injector cycle time and the machine acceleration time are determined by the short store regime and correspond to the present Tevatron cycle time and a ramp rate of about 20% that of the Tevatron.

Operating Characteristics. The operating characteristics of this machine show, not surprisingly, more dynamic variation than present day hadron colliders, *i.e.*, more electron like behavior. Figures 2(a)–(d) show an analytic estimate of the time evolution of the transverse emittance, bunch intensity, luminosity, and head-on beam-beam tune shift. In obtaining these results we have assumed no emittance growth mechanisms. The

Table 4: 30×30 TeV Workshop Parameters.

Parameter	Original	Modified
Beam Energy (TeV)	30	30
Initial Luminosity ($\times 10^{34}$ cm^{-2} s^{-1})	1.0	0.4
Injection Energy (TeV)	—	1
Number IRs	—	2
Dipole field (Tesla)	12.5	12.5
Circumference (km)	60	60
Number dipoles	—	3335
Initial transverse emittance, rms (mm-mr)		
Collisions	1.0 π	1.5 π
Injection	—	1.0 π
Initial longitudinal emittance, rms (eV-s)	—	0.5
Radio frequency (MHz)	—	360
rf voltage(MV)	—	25
Bunch length, rms (cm)	—	4
Bunch intensity ($\times 10^{10}$)	2.0	2.4
Bunches	12000	2030
Bunch spacing (ns)	25	100
Number of events/crossing (@60 mb, 1×10^{34})	11	60
Revolution frequency (kHz)	5	5
Initial beam lifetime burn off (hr)	75	16
Initial $\Delta\nu$ beam-beam head-on/IR	0.002	0.002
Crossing angle (μrad)	50	50
Initial $\Delta\nu$ long-range/IR	—	0.0039
β^* (cm)	50	20
Synchrotron radiation power/length/ring (W/m)	3.0	0.56
Total synchrotron radiation power/ring (kW)	151	29
Radiation damping time, FODO lattice (hours)		
Transverse	4.7	4.7
Longitudinal	2.3	2.3
Stored energy/beam (MJ)	1130	230
Filling time/ring (min)	—	10
Injector cycle time (min)	—	1
Acceleration time (min)	—	5
Injection dipole field (T)	—	4

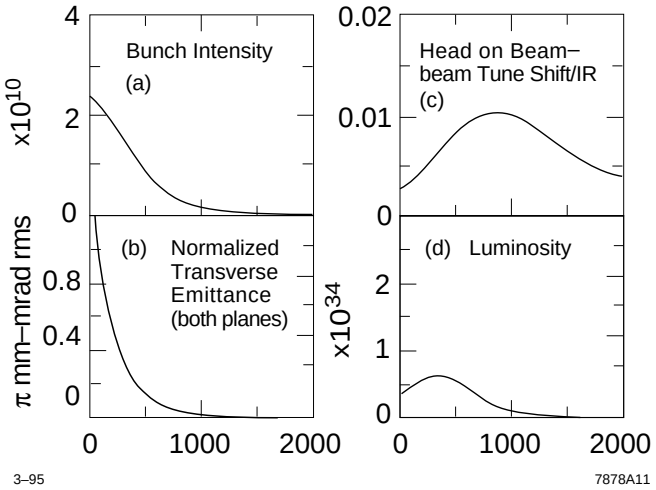

Figure 2: Time evolution of the store parameters for a dipole field of 10 T.

luminosity rises from an initial value of $\sim 5\times 10^{33}$ to $\sim 10^{34}$ over a period of $\sim$ 4 hours and then slowly falls again in a more or less symmetric fashion. The peak to average luminosity is a healthy 70% across this time span. During the 8 hour storage period the bunch intensity falls by a factor of 5 and the transverse emittance shrinks by an order of magnitude. The head-on tune shift increases with bunch density to $\sim$0.01/IR, but this is partially compensated by the reduction in long range tune shift which is not shown. The quite rapid fall in initial emittance intuitively leads one to suspect that the integrated luminosity is not strongly correlated to the assumed value for initial transverse emittance and other runs, not shown here, confirmed this. One interesting fact did emerge from this superficial exercise; initial emittances significantly less the 1 π result in a rapid saturation of the relaxed beam-beam tune shift limit *i.e.*this machine does not like very dense beams!

Other runs were performed with the same parameters using a 10 T dipole field (80 km circumference). With the reduced damping rate the luminosity peaks at a lower value and the optimum store length is longer but the same basic features are evident albeit at a $\sim$ 40% loss of performance. The lack of sensitivity to the dipole operating field is a healthy attribute given that we chose to use a "dipole" that is beyond the state of the art today. While these simulations were performed using a straight forward FODO lattice in the arc sections, the lattice working group demonstrated during the workshop enhanced damping lattices by manipulating the partition functions through the use of combined function magnets. Changing the partition functions from a FODO–like $J_x = J_y = 1.0$, $J_z = 2.0$, to a more desirable $J_x = J_y = 1.5$, $J_z = 1.0$, provides performance in the 10 T machine that is virtually identical to 12 T. Other techniques to

enhance the damping rate such as operating with a small momentum offset are also potentially attractive from this point of view.

Since we are relying for luminosity on the increased phase space density to counter balance the loss of bunch intensity, it is natural to be concerned about the effect of emittance dilution mechanisms. It is evident from the figures that a beam emittance which asymptotically approaches zero is nonphysical in the limit, and a more rational simulation would include beam heating mechanisms where the equilibrium beam emittance is defined by the balance between heating and cooling. Intrabeam scattering (IBS) is such a heating term which increases with increasing beam density. A first estimate of the impact of IBS was made by including a paramaterized IBS heating term in a self-consistent way. These results can be compared to those of Fig. 2 (a different calculation). As expected, there is little effect at the beginning of the store when the beam size is large, but it becomes progressively more important as the beam shrinks. The peak luminosity is reduced by $\sim 20\%$ and instantaneous luminosity falls off faster after the peak value with the transverse emittance approaching an asymptotic value of $\sim 0.15\pi$. This results in a 20% decrease in integrated luminosity over a 10 hour period. Maintaining the longitudinal emittance at its initial value of 0.5 eV-s by beam heating halves this decrease. While the effect of IBS is significant the overall features of the store evolution are similar.

Observations. Since magnets are a crucial and dominant feature of any accelerator in this energy regime it is appropriate to include some observations on this topic which are not strictly related to machine performance. While our basic machine model assumed a 12.5 T dipole it became apparent during the workshop that there is no threshold field necessary to enter the regime of usable emittance damping. All things being equal, the biggest impact on synchrotron radiation emission is operating energy, which produces the somewhat interesting observation that for a constant damping rate, the lower the dipole field the higher the operating energy, and vice versa. Alternatively, for a desired operating energy there is a maximum dipole field beyond which radiated power becomes prohibitive. These factors together with fiscal realities would indicate that optimistic but otherwise reasonable people would conclude that dipoles in the range of 9–15 T and a machine energy of 25–40 TeV can be made to fit into the basic conceptual framework outlined here. Beyond this regime a different approach is called for.

Magnet aperture and field quality are related quantities. As discussed in the other workshop reports, at the back-of-an-envelope level, a 5 cm magnet aperture would appear to suffice, including the needs of bore tube liners. Since field quality in the arc regions is invariably defined by the low energy performance of the magnets, the short dwell time (20 min) and 50% allowance for emittance growth in this model should permit a relaxation of SSC–like field quality specifications (factor of 3?) which in turn will reduce magnet costs. A 2-in-1 magnet style is also preferred for both cost implications and simplifications in the IR regions when the beams are brought into collision.

The use of high-T_c superconductors for the magnets does not appear to be necessary to achieve the magnet performance alluded to here. An elevated operating temperature (say, 10 to 15° K), while not necessary, is still highly desirable. The bore tube liner could become passive with no dedicated cooling circuits, a greater allowable temperature fluctuation across the magnet strings greatly simplifies the cryogenic system, as does the removal of radiated power at the higher temperature. Cryogenic operating costs are also reduced. High-T_c materials also raise the possibility of permitting an increase in the tolerable synchrotron radiation power density in the magnets, *i.e.*, a potential increase in luminosity. Since these items are, in principle, quantifiable, the basic elements for a cost/benefit study of a high-T_c magnet R&D program are available.

Conclusions. The possibility of utilizing synchrotron radiation emittance damping to enhance the performance, and simplify the construction, of a next generation hadron collider looks promising enough to warrant further attention. An operating energy in the range of 25–40 TeV would require 12.5 ± 3 T dipoles. Some form of magnet R&D program will be needed to support these aims.

3 Electron Linear Collider Facilities

3.1 Introduction

Over the past 6–7 years there has been a concerted effort to evaluate the physics which could be addressed with a future e^+e^- linear collider. This work was conducted in a series of workshops shown in Table 5. During the same period a series of Linear Collider Workshops was held to address the accelerator physics and technology of such a collider (see Table 6). These workshops served to disseminate information and provided an informal collaboration of R&D efforts at laboratories around the world. The result of these studies was a broad international consensus that the next e^+e^- collider should have an initial energy of about 500 GeV and should be expandable to 1 TeV and beyond. This conclusion evolved both from considerations of the technical difficulty of the linear collider and studies of the physics opportunities in this energy range.

Table 5: Physics Studies.

Date	Study	Location
1987	SLAC Study Group	US
—	La Thuile CLIC Study	Europe
1988	SNOWMASS	US
1989	First JLC Workshop	Japan
1990	SNOWMASS	US
—	Second JLC Workshop	Japan
1991	EE500 Workshops	Europe
—	Saariselka, Finland	International
1992	Colliding Beams Workshops (*ee*, *pp*, *ep*)	US
1993	Waikoloa, Hawaii	International
1995	Japan	Japan

A typical layout for such a collider is shown in Fig. 3. The key elements of the collider are highlighted:

- Electron and positron sources produce the beams
- Damping Rings shrink the beam size.
- Compressors and Pre-accelerators prepare the bunch for acceleration.
- The main linac accelerates the beam to high energy.
- The Final Focus demagnifies the beam size for collision.
- The detector must have a clean environment with low enough background for physics.

Although the basic features of the linear collider shown above are generic, the linear collider work around the world has led to several possible approaches.

To illustrate the range of the designs, a subset of parameters for colliders is shown in Table 7. (Parameter lists for all approaches are given later in this report). They illustrate the primary trade offs which can be made in order to obtain high luminosity at high energy. When beam-beam backgrounds are held roughly constant there are two ways to get high luminosity: (1) increase the power in the beam, or (2) decrease the vertical spot size.

As we move from TESLA to NLC/JLC, the beam power drops from 16.5 MW to 4.2 MW in the 0.5 TeV design and from 15.2 MW to 9.4 MW in the 1 TeV design. The vertical spot size in the 0.5 TeV designs also drops as we move to the right in Table 7 to keep the luminosity roughly constant. The situation for 1 TeV is somewhat different. Both TESLA and SBLC must drop the vertical beam size to the few nanometer range in order to keep wall power and beam-beam effects under control. The NLC/JLC design has a smoother scaling to 1 TeV, and can even be scaled to 1.5 TeV, as shown in Table 7.

The final energy of the linear collider can be obtained with two primary technological choices: superconducting or warm radio-frequency (rf) acceleration. The TESLA

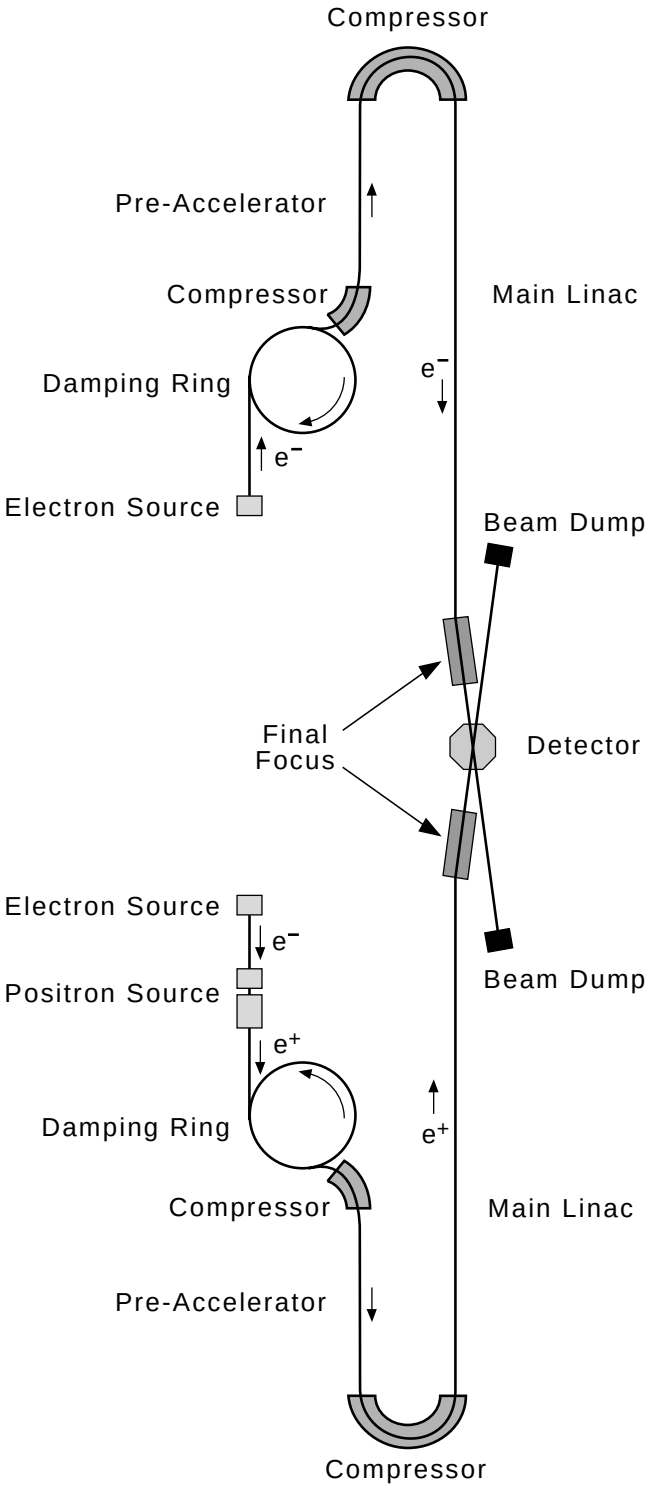

Figure 3: Schematic layout of a future e^+e^- Linear Collider.

collaboration is pursuing the superconducting approach. Within the warm category the S-band linear collider (SBLC) represents the lowest frequency option based on SLC technology developed about 30 years ago while the NLC ($\sim$ JLC) parameters shown in Table 7 push the accelerating frequency up by a factor of 4, which allows higher acceleration gradient.

Table 6: Accelerator Physics Workshops.

General Workshops:

Date	Workshop	Location
1988	LC88	SLAC
1990	LC90	KEK
1991	LC91	Protvino
1992	LC92	Garmisch
1993	LC93	SLAC
1995	LC95	KEK

Topical Meetings:

Date	Meeting	Location
1992	Final Focus and Interaction Region	SLAC
1992	Damping Rings	KEK
1993	Emittance Preservation	KEK
1994	e^+e^- Sources	DESY
1994	RF Power Sources	BNL

Although all designs shown here have 0.5 TeV lowest energy, it is, in general, not a problem to drop the energy to the Top threshold with some modest loss of luminosity. Note that a single 1.5 TeV parameter set is given for NLC. This parameter set was prepared at the request of other working groups and evolved from studies several years ago by the SLAC parameters group to evaluate several designs as to energy flexibility. This analysis showed that the NLC/JLC designs can cover the 0.5–1.5 TeV range. Another high-energy design was produced by CLIC for 2 TeV; however, recently they have focused on the 0.5 TeV design. The other designs shown in Table 3, however, have not been extended to 1.5 TeV.

Before beginning it is useful to note that as we have learned more from the technology development and SLC experience, the designs in this report have evolved. Although this evolution is still taking place, the designs and the enabling techniques are reaching maturity now.

To begin the detailed discussion, we present a summary of the SLC to set a baseline for future designs. Although at first look the SLC is a rather specialized hybrid collider, in fact, the SLC is addressing all of the key issues that are being studied for future colliders. The third section presents an overview of linear collider R&D and introduces the parameters sets and main features of all the designs. The next five sections each discuss a particular design and/or the associated test facilities that are under development. Finally, the report summary discusses world collaboration.

3.2 The SLAC Linear Collider Program

3.2.1 The SLAC Linear Collider [5]

The SLAC Linear Collider (SLC) holds a unique place in the field of high energy accelerators as the world's first electron-positron linear collider. By the early 1980's, it was evident that the previous generation of electron-positron storage ring accelerators could not practically be extended beyond the energy range of LEP and LEP 2. The circumference, and hence cost, of an electron storage ring scales like the square of the energy making a 0.5–1.0 Tev machine prohibitively expensive. Linear colliders scale linearly with energy and can potentially provide higher energy at lower cost. The SLC was proposed as both a prototype for a new generation of electron accelerators and as an inexpensive entry into the physics available at the mass of the Z. Because it was the first example of a new accelerator technology, it was a particularly difficult machine to understand and commission. It was almost 2 years from the completion of construction in 1987 until the first Z event was seen by the Mark II detector on April 11, 1989. Several more years of effort were required to develop the knowledge and experience to operate the first linear collider reliably. Today the success of the SLC has generated widespread interest in linear colliders throughout the international accelerator community. Close collaboration between the SLC and other linear collider groups has been of great benefit to both efforts.

A cycle of the SLC begins with two electron bunches stored in the north damping ring and two positron bunches stored in the south ring. Each 1/120 second, one positron bunch and both electron bunches are kicked out of the rings and accelerated down the linac. The positrons, followed by the first electron bunch, are accelerated to about 47 GeV before they are separated by a dipole magnet at the end of the linac, transported around the collider arcs and brought into collision. These bunches then travel back through part of the beam line until they are ejected into extraction lines to beam dumps. The second electron bunch is deflected onto a target two-thirds of the way down the linac to produce the next bunch of positrons. The positrons from the target are collected, accelerated to 200 MeV and transported back to the beginning of the linac. There they are joined by two bunches of electrons from the source, accelerated to 1.2 GeV and stored in the two damping rings for the next cycle.

Table 7: Comparison of Linear Collider Parameters

Parameter	TESLA		SBLC		NLC (~JLC)		
Center-of-mass energy (TeV)	0.5	1	0.5	1	0.5	1	1.5
Luminosity (10^{33})	7	10	4	6	8	20	19
Repetition rate (Hz)	0	5	50	50	180	120	120
Bunches/rf pulse	800	4180	125	50	90	75	75
N (10^{10})	5.15	0.91	2.9	2.9	0.65	1.3	1.3
x/y emittance (10^{-8} m)	2000/100	520/6.3	1000/5	1000/10	500/5	500/5	500/5
x/y beta at IP (mm)	25/2	20/1	22/0.8	32/0.8	10/0.1	40/0.1	40/0.1
x/y sigma at IP (nm)	1000/64	325/8	670/28	572/9	300/3	425/2	425/2
Bunch length (microns)	1000	500	00	500	100	100	100
Upsilon	0.029	0.058	0.055	0.091	0.096	0.28	0.42
Pinch enhancement	2.3	2	1.6	1.7	1.4	1.4	1.3
Beamstrahlung delta	0.03	0.03	0.03	0.07	0.03	0.08	0.10
Number photons/e^-	2.7	1.3	2	2.3	0.9	1.1	1.1
Loaded gradient (MV/m)	25	25	17	34	37	74	74
Linac length (km)	20	40	29.4	29.4	14 1	4	21
Number klystrons	1202	2404	2450	4900	1890	3850	5820
Klystron peak power (MW)	3.25	3.25	150	150	96	105	105
Pulse compression gain	—	—	—	2	3.6	6.6	6.6
Power/beam PB (MW)	16.5	15.2	7.3	5.8	4.2	9.4	14
AC power PAC (MW)	137	159	114	200	92	144	218
$2P_B$/PAC	0.24	0.19	0.13	0.06	0.09	0.13	0.13

3.2.2 Polarized Beams at the SLC

The first SLC polarized source, using a bulk GaAs cathode illuminated by a dye laser operating at 715 nm, produced a polarization of 27–29%. In 1993 both the cathode and the laser were upgraded for higher performance. A new Ti:Sapphire laser pumped by a doubled YAG laser has a hundred times more power and a tuneable wavelength.

The present cathode uses a "strained lattice" technology to achieve higher polarization. In a bulk GaAs photocathode the laser light excites electrons from two degenerate energy levels. The electrons from these two levels have different polarizations which partially cancel, giving a maximum achievable polarization of 50%. For the strained lattice, a 100–300 nm layer of GaAs is grown on a GaAsP substrate. Because the GaAs layer is thin, its lattice distorts to match the GaAsP lattice. With long wavelength laser light (typically 865 nm), only one of the two energy levels is excited and polarization up to 90% can be attained.

The major surprise was a large anomalous spin precession through the north arc. At the energy of the Z, the arc vertical betatron tune is very nearly equal to the spin tune causing a resonance-like behavior. Small changes in the vertical trajectory can strongly affect the spin orientation. This effect also causes a few percent depolarization due to the different paths followed by particles of slightly different energy. New feedback systems to better control the beam trajectory through the arc have allowed stable delivery of polarized electrons. The extreme sensitivity of polarization to vertical orbit has also allowed the development of techniques for using controlled oscillations to optimize the spin orientation and to minimize the depolarization effects. The polarized source has proven very reliable with over 95% availability during more than two years of operation. For the 1994 run, a thin (100 nm) strained lattice cathode was installed to provide about 80% polarization. A larger area cathode configuration has also been developed to support higher beam intensity.

Further research on cathode technology is aimed at even higher polarization for future runs.

3.2.3 Luminosity

The luminosity of a linear collider is given by the formula

$$L = \frac{N^+ N^- f H_d}{4\pi\sigma_x\sigma_y}\eta \qquad (1)$$

where N^+ and N^- are the number of positrons and electrons per bunch, f is the collision frequency, σ_x and σ_y are the horizontal and vertical beam sizes at the collision point. The H_d is an enhancement factor due to disruption which describes the additional focusing of one bunch by the field of the other bunch during the collision. The efficiency factor, η, relates the peak luminosity to the average luminosity delivered over a period of weeks. This formula clearly indicates the strategy for increasing the luminosity: for fixed collision frequency, one must increase the number of particles per bunch and/or decrease the beam area. To translate gains in peak luminosity into an increase in total events, the efficiency is a critical factor. Progress at the SLC has been made in all parameters but the biggest payoff has come from smaller bunch size and more efficient operation.

The SLC polarized electron source and the positron production system are capable of producing 4–5 $\times 10^{10}$ particles per bunch but the maximum operational intensity has been limited by constraints on stability and on non-linear effects which increase the beam size. In 1993, the intensity was limited by the onset of a bunch length instability in the damping rings at a threshold of 3×10^{10} particles per bunch. The instability is caused by the interaction of the intense bunches with the impedance of the vacuum chamber, primarily due to sharp transitions in its shape. For the 1994 run, smoother vacuum chambers have been constructed for both rings. This has raised the threshold for turbulent bunch lengthening by a factor of 1.5 to 2, well beyond other practical limits on the SLC beam intensity. Stable operation at 4×10^{10} particles per bunch has already been established.

Producing high-current, low-emittance beams and transporting them without increasing the emittance is one of the most difficult challenges of a linear collider. The history of emittance reduction in the SLC is an excellent example of the development of the technology required for linear colliders through successive refinements in measurement and control techniques. Throughout the SLC, the basic strategy is to match the bunch as well as possible theoretically, then measure the residual error and compensate for it by introducing a deliberate error to cancel it exactly. Precision, non-invasive diagnostics are required to measure and match the beams through the transport lines and to accelerate them down the Linac with minimal emittance growth. Careful alignment and orbit control are required to prevent wakefield growth in the copper accelerating structure, where the fields induced by the head of the bunch can deflect the tail and distort the bunch along its length. Residual wakefield tail can be minimized by using a controlled oscillation to generate errors which exactly cancel the measured tails. Emittances better than the original design value have been achieved for both electrons and positrons at the end of the linac

At the end of the 1992 run, a new operating mode with flat beams (vertical size much smaller than horizontal) was tested in preparation for the Final Focus Test Beam, a linear collider development project. Flat beams have the advantage of a smaller beam area, which produces higher luminosity. It is easy to create a small vertical beam size in the damping rings; the challenge is in preserving it. The original SLC design had relied on operation with round beams because of the difficulty of controlling the vertical-to-horizontal coupling in transport lines such as the arcs. In the brief test run, beam size ratios of 10:1 were easily achieved out of the damping rings and the long years of effort in developing techniques to control the beams throughout the SLC allowed the very small vertical size to be delivered for collisions. The luminosity doubled almost immediately. Flat beam operation was successfully commissioned early in the 1993 run. In this configuration, the beams can be focused to a size of 2.1 μm horizontally and 0.8 μm vertically was achieved. The corresponding bunch area of 1.7 square μm is significantly smaller than the SLC design goal of 2.9 square μm. (See Fig. 4.)

For the 1994 run, the final focus was upgraded further to take full advantage of flat beam operation. With roughly equal horizontal and vertical emittances as in the original SLC design, the beam size at collisions is dominated by the linear size due to the emittance. With a very small vertical emittance, this is no longer true and the contribution to the beam size from residual chromatic aberrations is much larger than the linear size. Additional quadrupole and sextupole magnets have been installed to reduce these aberrations and improve tuning flexibility. New wire scanners in each final focus provide more precision diagnostics. With these improvements, the SLC has been able to focus a low current beam to a vertical beam size of less than 500 nm, one third of the original design. This provides a factor of two increase in the peak specific luminosity. The challenge is to reach and maintain these small beam sizes at operating intensity. (See Fig. 5.)

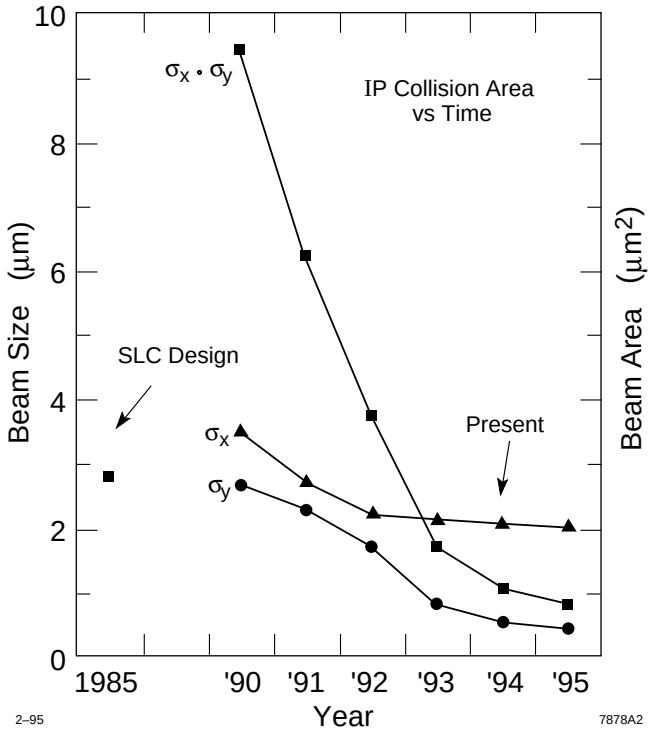

Figure 4: The evolution of SLC IP beam size versus time.

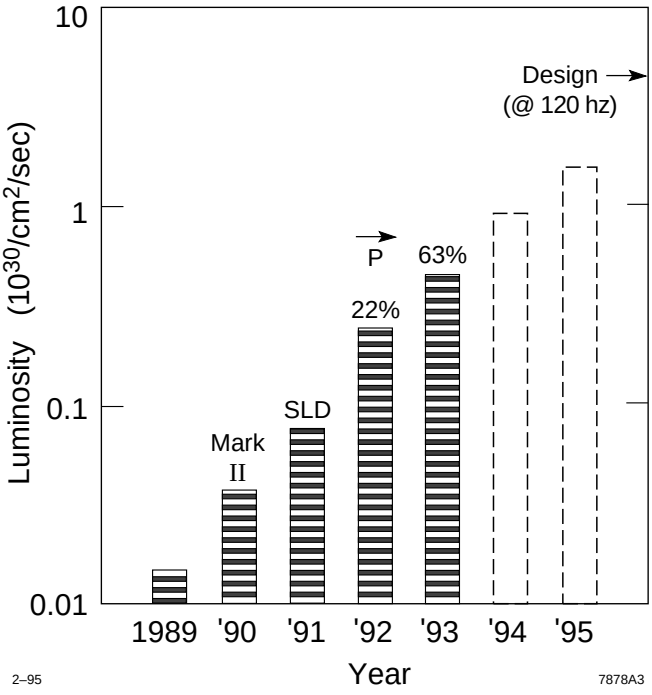

Figure 5: SLC peak luminosity.

3.2.4 Efficiency

The final important factor affecting the event rate is the machine operating efficiency, which has steadily improved to an average of 60–70%. While hardware reliability is essential, the major advance in SLC operations has come from the development of an extensive network of feedback systems to stabilize the bunches throughout the machine. In contrast to a storage ring, a linear collider is not inherently stable and is extremely dependent on feedback and other controls for reliable operation. The basic SLC feedback systems provide pulse-to-pulse control of beam energy and trajectory with special applications for the polarized source and other critical components. There are more than 50 feedback systems active during SLC operation, controlling over 200 parameters.

3.2.5 Future Plans

Motivated by the success of the polarized electron source and by the increase in luminosity, SLAC has completed two major improvement projects aimed at maintaining a vital SLC physics program for the next few years. For the 1994 run, new damping ring vacuum chambers and a major upgrade of the final focus magnet system have been installed to support higher beam intensity and smaller beam size. For these parameters, the focusing of one bunch by the field of the other can become significant, producing up to 30% higher luminosity. The first observation of the long-predicted disruption enhancement would be an exciting achievement.

These upgrades are expected to produce an overall factor of 2 to 4 increase in luminosity compared to 1993 after they are fully commissioned. In the 1994 run, SLD should log more than 100K Zs with 80% polarization to improve the measurement of the weak mixing angle by a factor of two. In future runs with the new SLD vertex detector installed, the goal is more than 500 thousand Zs with over 80% polarization in the next four years. This will provide the highest precision measurement of the Weinberg angle and important B physics results.

In the ten years since construction began on the SLC, the interest in linear colliders has grown enormously. Today most of the major high-energy physics laboratories in the world have active linear collider development programs. Tremendous progress has been made in understanding the techniques required to build and operate this new kind of particle collider. The SLC remains in the forefront of these efforts as the only existing linear collider where new ideas and techniques can be tested. Its recent success with high polarization and increased luminosity has given new impetus to plans for the next linear collider. The SLC has conclusively demonstrated that linear colliders are the way to reach the TeV scale in electron-positron accelerators.

3.3 An Overview of Future e^+e^- Linear Collider Designs [6]

The parameters of linear colliders with $E_{\rm c.m.} = 0.5$ TeV based on a compilation made by G. Loew at the LC–93 Conference is given in Table 8. These colliders are:

- TESLA which is based on superconducting rf. All the others would use room temperature rf.
- {SBLC which uses S-band (3 GHz) rf where there is extensive operating experience.
- NLC which uses higher frequency X–band (11.4 GHz) rf in a modulator-klystron-accelerator configuration similar to S–band linacs.
- JLC–I which has three frequency options, S–band, C–band (5.7 GHz), and X–band. Multiple bunches are accelerated in each rf pulse as they are in TESLA, SBLC, and NLC.
- VLEPP which employs a single high-intensity bunch rather than multiple bunches.
- CLIC which is a two-beam accelerator with klystrons replaced by an rf power source based on a high-current, low-energy beam traveling parallel to the high-energy beam.

3.3.1 Beam Power and Spot Size

The luminosity is given by

$$L = \frac{1}{4\pi}\frac{N^2 f_c}{\sigma_{x0}\sigma_{y0}}\, H_D = \frac{1}{4\pi}\frac{N^2 f_c}{\sigma_x \sigma_y}, \qquad (2)$$

where N is the number of particles/bunch and fc is the collision frequency. Focusing during the collision, disruption, can be accounted for by an enhancement factor H_D in the left-hand expression where the beams sizes without disruption σ_{x0}, σ_{y0} are used or by using the disrupted beam sizes σ_x, σ_y as in the right-hand expression.

The electromagnetic fields at the collision point are paramaterized by

$$\Upsilon = \frac{5 r_e^2}{6\alpha}\,\frac{\gamma N}{\sigma_L(\sigma_x + \sigma_y)}, \qquad (3)$$

where field enhancement is approximately accounted for by using the disrupted sizes. The energy in units of mc^2 is denoted by γ, and σ_L is the bunch length. The mean beamstrahlung energy loss $\delta_B \propto \Upsilon^2$ and backgrounds from beamstrahlung, e^+e^- pairs, and hadronic events depend on Υ. When $\Upsilon \ll 1$ and $\sigma_x \gg \sigma_y$, the mean number of beamstrahlung photons per incident particle is

$$n_\gamma \approx \Upsilon\frac{5\alpha\sigma_L}{2 r_e \gamma} \approx \frac{2\alpha r_e N}{\sigma_x}. \qquad (4)$$

n_γ serves as an approximate measure of backgrounds.

The luminosity can be rewritten in terms of four parameters: γ, n_γ, σ_y, and the beam power, $P_B = N f_c \gamma mc^2$

$$L \approx \frac{1}{8\pi\alpha r_e mc^2}\,\frac{P_B n_\gamma}{\gamma\sigma_y}. \qquad (5)$$

Detector backgrounds fix n_γ, and the center-of-mass energy determines γ. The trade-off is between beam power and spot size. Roughly speaking, TESLA and SBLC would have high beam powers and large spots while the others would have small beam powers and small spots. "Large" and "small" are relative to each other; all of these colliders have large beam powers and small spots compared to present day practice at the SLC.

3.3.2 Multiple Bunches

All designs except CLIC and VLEPP use multiple bunches to achieve good energy efficiency. The cost of filling the accelerator structure with rf energy is amortized over a large number of bunches rather than a single bunch. Using multiple bunches has implications for both the fundamental and higher modes. Each bunch needs roughly the same energy profile down the linac to avoid emittance blow-up from dispersive effects, and they need to have the same energy in the final focus to minimize chromatic aberrations. Bunch train lengths and accelerator structure filling times are comparable, and the accelerator must be prefilled and the rf amplitude ramped so that each bunch gains the same energy

The long-range transverse wakefields from higher modes can cause emittance blow-up that is in addition to that from short range wakefields. The higher modes must be damped or detuned (spread out in frequency) to reduce these wakefields to acceptable levels.

The dominant multibunch effect in TESLA is associated with chromatic effects from the bunch-to-bunch energy spread. A systematic spread could be caused by effects such as Lorentz detuning where the cavity dimensions change during the pulse due to the pressure from the stored electromagnetic energy. With a bunch-to-bunch energy spread of 10^{-3}, the emittance increase is a factor of ten. This results in a tight tolerance of a few times 10^{-4} on the energy spread.

Two of the designs, VLEPP and CLIC, are not designed for multiple bunches. VLEPP has a large, single bunch, and requires stringent tolerances on the linac for emittance preservation and a novel final focus that employs a traveling focus. The possibility of using up to

Table 8: Selected Linear Collider Parameters for $E_{\rm c.m.} = 0.5$ TeV (G. Loew, Linear Collider 93), where VLEPP employs a "traveling focus." The loaded gradient is calculated before applying further reductions for off-crest running, BNS damping, etc., VLEPP excluded. The AC power is calculated only for the linac damping ring, detector, utility power, etc., and power for klystron focusing are not included [SBLC bases its number on a combined klystron-modulator efficiency of 45%, JLC and NLC have assumed this number to be closer to 35%, and SLED–I (for JLC–I(S)) and SLED–II (for JLC–I(C), JLC–I(X), NLC, and VLEPP) are assumed to be 65% efficient].

Parameter	TESLA	SBLC	JLC-I (S)	JLC-I (C)	JLC-I (X)	NLC	VLEPP	CLIC
L (10^{33} cm^{-2} s^{-1})	7	4	4	7	6	8	15	2–9
rf frequency (GHz)	1.3	3.0	2.8	5.7	11.4	11.4	14	30
Repetition rate (Hz)	10	50	50	100	150	180	300	1700
Bunches per rf pulse	800	125	55	72	90	90	1	14
N (10^{10})	5.15	2.9	1.30	1.0	0.63	0.65	20.	0.6
BPM precision (μm)	10.	10.	NA	NA	1.	1.	0.1	0.1
$\gamma\epsilon_x$ / $\gamma\epsilon_y$ (10^8 m)	$\frac{2000}{100}$	$\frac{1000}{50}$	$\frac{330}{4.5}$	$\frac{330}{4.5}$	$\frac{330}{4.5}$	$\frac{500}{5}$	$\frac{2000}{7.5}$	$\frac{180}{20}$
β_x^* / β_y^* (mm)	$\frac{25}{2}$	$\frac{22}{0.8}$	$\frac{10}{0.1}$	$\frac{10}{0.1}$	$\frac{10}{0.1}$	$\frac{10}{0.1}$	$\frac{100}{0.1}$	$\frac{2.2}{0.16}$
σ_{x0} / σ_{y0} (nm)	$\frac{1000}{64}$	$\frac{670}{28}$	$\frac{300}{3}$	$\frac{260}{3}$	$\frac{260}{3}$	$\frac{300}{3}$	$\frac{2000}{4}$	$\frac{90}{8}$
σ_L (mm)	1000	500	80	80	67	100	750	170
IP crossing angle (mrad)	0	3	7.3	8	7.2	3	—	1
Υ	0.029	0.055	0.24	0.21	0.16	0.096	0.074	0.35
Disruptions, D_x / D_y	$\frac{0.54}{8.5}$	$\frac{0.36}{8.5}$	$\frac{0.13}{13}$	$\frac{0.13}{11.7}$	$\frac{0.07}{6}$	$\frac{0.08}{8.2}$	$\frac{0.4}{215}$	$\frac{1.3}{15}$
H_D	2.3	1.6	1.6	1.5	1.7	1.4	1.3	3.3
δ_B	0.03	0.03	0.10	0.08	0.05	0.03	0.13	0.36
n_γ	2.7	2.0	1.6	1.4	1.0	0.9	5.0	4.7
Unloaded gradient (Mv/m)	25	21	22	40	40	50	108	80
Loaded gradient (MV/m)	25	17	19	33	31	38	96	78–73
Active linac length (km)	20	29.4	28	16.7	17.7	14	6.4	6.6
Section length (m)	1.04	6	3.6	2	1.3	1.8	1.01	0.273
Number of sections	19232	4900	7776	8360	13600	7778	5200	24000
Number of klystrons	1202	2450	1944	4180	3400	1945	1300	2
Klystron peak power (MW)	3.25	150	85	45	70	94	150	700
Klystron pulse length (μs)	1300	2.8	4.5	3.6	0.84	1.5	0.7	0.011
Pulse length to section (μs)	1300	2.8	1.2	0.6	0.21	0.25	0.11	0.011
Pulse compression/gain	—	—	2.4	4.2	3.2	4	4.22	—
a/λ (input/output cavity)	0.15	0.15/0.11	0.13	0.16/0.12	0.24/0.14	0.22/0.15	0.14	0.2
P_B (MW)	16.5	7.3	1.4	2.9	3.4	4.2	2.4	.4–1.6
AC power (MW)	137	114	106	193	86	141	91	175
$2P_B/P_{AC}$	0.24	0.13	0.03	0.04	0.09	0.06	0.05	0.02

four bunches in CLIC is still under study, with the issues being energy compensation and control of intrabunch transverse wakefields.

3.3.3 Radio Frequency Power

Most of the colliders in Table 8 require a large number of high peak-power klystrons. S–band klystrons delivering 80 MW peak power for 4.5 μs are in operation at the KEK Accelerator Test Facility. This is essentially the performance assumed for JLC–I (S). A 150 MW, 3.0 μs klystron developed by SLAC and DESY for the DESY SBLC and S–band preaccelerators of the NLC has recently operated at full power and will be used in a test facility at DESY. X–band klystrons have operated at KEK with the latest tube reaching an output power of 70 MW in 50 ns pulses with 35% efficiency. At SLAC, two X–band klystrons have reached a power over 50 MW with an output pulse duration of 1.5 μs and an efficiency of about 40%.

The efficiency for transforming AC wall plug power to rf power is one of the major factors determining the economics of linear colliders. This efficiency has two major contributors, the modulator and the klystron. The need to improve modulator efficiency has led to a number of ideas, including a Blumlein configuration for the pulse-forming network that has been successfully tested at KEK and the use of a high voltage switch tube rather than a pulse transformer being pursued for SBLC. This has proven to be more difficult than anticipated, and switch tubes are now a backup to conventional modulators in the SBLC test linac.

It is impractical to directly generate the short rf pulses needed for the high-frequency colliders. A substantial fraction of modulator inefficiency comes from the rise- and fall-times of the pulse transformer that steps-up the output voltage. Pulse compression matches a long klystron pulse at a reduced peak power to the short bunch trains and accelerator structures that are appropriate for high-frequency rf. SLED–II pulse compression has been tested with 50 MW, $\sim$ 1 μs input pulses, and power gains of 3.6 to 4.1, with efficiencies of 60–68% have been demonstrated. The intrinsic efficiency of this design is 70–75%. With improved components, this is expected to reach a power gain of 4.2 to 4.6 with 66–70% efficiency.

TESLA has unique power source requirements. The high-Q cavities and long pulse length reduce the peak power to 3.25 MW, but the modulator must be capable of delivering that power for over a millisecond.

The two-beam accelerator, personified by CLIC in Table 8, avoids the thousands of individual rf power sources by replacing them with a high-current, low-energy drive beam. This low-energy beam has a time structure appropriate for generating 30 GHz rf. It is accelerated by a 350 MHz superconducting rf system, and energy is extracted with transfer structures spaced roughly 1.5 m apart. Drive beam generation is under study at the CLIC Test Facility, where single, 8 bunch, and 24 bunch pulse trains have been produced and—using a CLIC section as the transfer structure—56 MW of rf power has been generated. This corresponds to a peak decelerating field in the last cell of 107 MV/m. When this power was transferred to the accelerating section an average accelerating field of 71 MV/m was seen with no signs of breakdown.

3.3.4 Accelerator Structures

Room temperature accelerators are performing with gradients close to those listed in Table 8. Precision machining is being used for tight fabrication tolerances and for the surface qualities needed for high gradients. Structures are being made at KEK and CERN using direct copper-to-copper diffusion bonding of precision machined cells. A CERN–made 11 GHz structure has been tested at KEK and exceeded 100 MV/m accelerating field after a reasonable amount of conditioning. Its performance was limited by the available rf power. A full-length NLC section has reached over 55 MV/m in a high-power test, and, as mentioned above, a 30 GHz CLIC structure has shown excellent performance. Costs for mass fabrication are not excessive.

High-power pulsed processing is having continuing success in raising the gradient of superconducting cavities, with a gradient of 25 MV/m being reached in a five-cell, 1.3 GHz cavity. Demonstrating this type of behavior in a larger scale linac, together with reducing costs, are major goals of the TESLA Test Facility under construction at DESY.

3.3.5 Emittance Preservation

The vertical invariant emittances $\gamma\epsilon_y$ are small, and emittance preservation during acceleration is a central consideration. Emittance growth caused by the combination of injection jitter and wakefields must be controlled by tight tolerances on injection elements and BNS damping.

Misalignments of the accelerator sections, quadrupoles, and beam position monitors in the main linac cause emittance growth through wakefields and dispersion different central trajectories for different energies. Beam based orbit correction procedures, where optical elements are varied and orbit changes measured, have become almost universally adopted as the way to loosen alignment tolerances. Experience is being gained at the SLC where these technologies are used to control emittance dilution.

3.3.6 Center-of-Mass Energy ($E_{\rm c.m.}$) greater than 1 TeV

The discussion above concentrated on $E_{\rm c.m.} = 0.5$ TeV, but there is substantial interest in higher center-of-mass energies. Ideally the luminosity would increase as ($E^2_{\rm c.m.}$) to reflect the decrease in the cross section for production of point-like particles. Table 7 in the Introduction gives recent parameters for upgrades of TESLA, SBLC, and NLC to 1 TeV (and 1.5 TeV for NLC).

The two ways to reach 1 TeV are to double the length, or double the gradient by quadrupling the peak power using a combination of increasing the number of klystrons, the klystron peak power, and the pulse compression gain. The former is used in TESLA since 50 MV/m would be near the fundamental gradient limit of superconducting rf in Nb. The latter is used in SBLC and NLC. The threshold for rf capture of dark current is about 20 MV/m at 3 GHz and about 80 MV/m at 11.4 GHz. The SBLC gradient is well above that threshold, but may be reached with appropriate attention to surface preparation and with RF processing. The NLC gradient is below the dark current limit and has been easily exceeded in the test mentioned above.

A straightforward application of either method of doubling the energy leads to unacceptable AC power consumption, so the parameters have changed to reflect this. First, the luminosity has not been scaled as $E^2_{\rm c.m.}$. Second, the trade-off between high beam power and small spots (Eq. (5)) is no longer the central theme it was in the 0.5 TeV discussion. All of the parameter lists have evolved in the direction of small spots, with nearly identical invariant emittances. The underlying assumption for TESLA and SBLC are that after gaining experience with correction and optimization procedures, the vertical emittance can be reduced by an order of magnitude. This is possible if the accelerator complex has been designed and constructed with the goal of producing small emittances.

The 1 TeV NLC parameters show a third approach to the problem of AC power consumption. They are based on improved efficiency. Some of that improvement has come from evaluating the modulator, klystron, and pulse compression efficiencies for the $E_{\rm c.m.} = 0.5$ TeV collider. The current estimate is that the AC power for the linac would be 92 MW versus the 141 MW at LC–93. Additional efficiency improvements are counted on for 1 TeV. These may include elimination of modulators through using a gridded klystron or a cluster klystron.

3.4 The Japanese Linear Collider (JLC) and Accelerator Test Facility (ATF) [7]

3.4.1 Basic Design Approach

The Japanese Linear Collider (JLC) design is based on normal-conducting linac technology in order to save R&D time for construction of a TeV linear collider. The wall plug power was assumed to be a few hundred MW at largest. The linac gradient was set to be at almost 100 MV/m. In order to achieve a luminosity of the order of 10^{34} cm^{-2} s^{-1} with those parameter constraints, X–band ($\sim$ 10 GHz) was chosen for the main linac frequency. Since the X–band linac technology was quite immature, the top priority was to develop it by extending the well established S-band technology.

An Accelerator Test Facility (ATF) was founded at KEK in 1988 in order to promote linac R&D work. At first an S–band rf system was established with several 5045 klystrons sent from SLAC. High gradient tests were carried out for S–band structures. Based upon this infrastructure, R&D work for X–band linac technology was at once started. Thereby efforts have been devoted mostly to develop X–band klystrons of 100 MW class. High-gradient tests of X–band structures also were carried out, as klystrons of a few tens of MW became available.

In the course of the X–band work and miscellaneous studies, the main purpose of the ATF gradually became construction of a test damping ring. Its energy was chosen to be 1.54 GeV. The injector is an S–band linac of the same energy. Construction of the accelerator complex was started in 1991. The ring is expected to provide electron bunches with their normalized emittance as small as a required value of 5×10^{-8} rad m.

Theoretical design work has been developed in order to optimize general parameter sets for the JLC, along with the above experimental work. The basic guideline has been to adopt a multibunch scheme per linac pulse and a small-crossing-angle collision. Major results in this field are: 1) study of the beam behavior at the collision which enables accurate evaluations of the luminosity, 2) study of achromatic final-focus optics which enables a large momentum acceptance, 3) detailed estimation of background noises, and 4) study of beam break-up and beam loading in the main linac.

3.4.2 Critical Issues for the Main Linac

Total Wall-Plug Power. The total power would certainly be within the above constraint for $E_{\rm c.m.} = 0.5$ TeV with parameter sets presently under consideration, but it would be necessary to reduce the repetition rate and the expected luminosity for $E_{\rm c.m.} = 1$ TeV or higher, since the total power is approximately proportional to $E_{\rm c.m.}$

Radio Frequency Power Source. Desirable ratings for the klystron output are 130 MW, 500-ns-long pulses per tube. Presently available tubes provide $\sim$ 70 MW, 100 ns pulses. Development of reliable output windows is the key issue in order to achieve these ratings. Due to large

power consumption, the conventional focusing solenoid should be replaced—*e.g.*, by a superconducting one.

In order to attain required gradients in the main linac, at least one-fold compression of the klystron output power is necessary, with the peak power doubled thereby. It should be tested to see whether amplitude or phase modulations brought about in the process are tolerable for an identical acceleration of each bunch.

The high-voltage pulse should have rise/fall times short enough compared with the pulse length of 500 ns in order to improve the overall power efficiency. A modulator with a Blumlein PFN seems promising, since the step-up ratio of a pulse transformer can then be halved, leading to a considerable shortening of its time constants. Capacitors with the smallest possible intrinsic inductance are also a necessary ingredient for the PFN in order to ensure fast ramping times.

Structure. High-gradient tests were carried out to verify the feasibility of required gradients 50 to $\sim$ 100 MV/m with an X–band structure. The gradients seem attainable, but the conditioning time was an order of magnitude longer than SLAC and CERN structures. Study for treatment of the structure surface is an immediate problem.

The X–band structure needs to be fabricated very accurately. Fine machining of structure pieces must be well established in order to attain dimensional accuracies on the order of 1 μm or better. Progress is yet only midway, however, toward bonding the pieces into a structure with a tolerable loss of the accuracies and with good electric and vacuum contact. A diffusion bonding technique is being developed for this purpose.

In order to damp the HOM effect, simulation studies have been carried out for both damped and detuned structures. A reasonable set of dimensions was found for a damped structure with four circumferential slots, although its fabrication may be cumbersome. Concerning a detuned structure, a new method was developed to calculate the dispersion relations of HOM modes up to the order of 20 or higher. Wakefields would then be calculated with a good accuracy for the multibunch case. It is urgently necessary to establish some facility (such as the Next Linear Collider Test Accelerator (NLCTA) at SLAC) to carry out beam measurements of the wake and check the validity of simulations.

Technology for accurate beam monitoring and alignment system for miscellaneous linac elements should be developed in this experimental work.

3.4.3 Injector for the Main Linac

Electron sources. Conventional cathodes can provide sufficient electrons per bunch for the JLC design, but it is not yet clear how uniform the population should be among the bunches in a train. This should be estimated carefully in order to control the BBU in the main linac. In this respect, a conventional grid-controlled thermionic gun might be inadequate, and an rf gun might be needed.

As a polarized electron source, GaAs photocathodes have come into practical use. The issue at present would be to incorporate the cathodes in an rf gun system.

Damping Ring. The damping ring must provide beams with the small vertical emittance given above with a repetition rate as high as 150 Hz. A lattice of FOBO type seems promising to attain the low emittance according to simulations. A long wiggler magnet section is necessary to ensure a fast damping time. The specifications are much more stringent than those for conventional rings; therefore, it is quite desirable to verify the feasibility by constructing a test ring. A fine alignment system for magnets is a key ingredient, since the coupling between vertical and horizontal betatron oscillations should be minimized to achieve the low emittance. The emittances, both transverse and longitudinal, should be as uniform as possible among the bunches for the beam dynamics in the main linac. For this sake, the ring rf system must comprise damped cavities and energy-compensating cavities. Those technologies will be developed in the ATF damping ring.

Beam Transport and Bunch Compression. Every bunch should be equally extracted from the ring. Hence, two kicker magnets, spaced by a π phase and driven by a common power unit, will be used to cancel the effect of ripples in a driving pulse.

The bunch length σ_z should be about 60 μm, while it is about 3 mm; in the ring, therefore, a bunch compressing line should be very carefully designed. Emittances should not grow in the line. Furthermore, a uniformity among the bunches is necessary also for this compressing process.

3.4.4 Interaction Region

Final Focus. The optics should be such that: 1) it includes a collimator to reject too many off-momentum particles, which might otherwise cause background noises at the collision point; 2) the achromatic correction should be sufficient to keep the beam size small at the collision point, and 3) the bore aperture of the final quadrupole magnet should be large enough to avoid an emittance growth due to image currents on the pole surfaces.

The final quadrupole magnet is the most technically difficult element. The poles should be machined with an accuracy of about 1 μm. A 1 m model was fabricated, and has been successfully used at the FFTB line. However, for the JLC, it would have to be at least a few meters long, making the machining much more

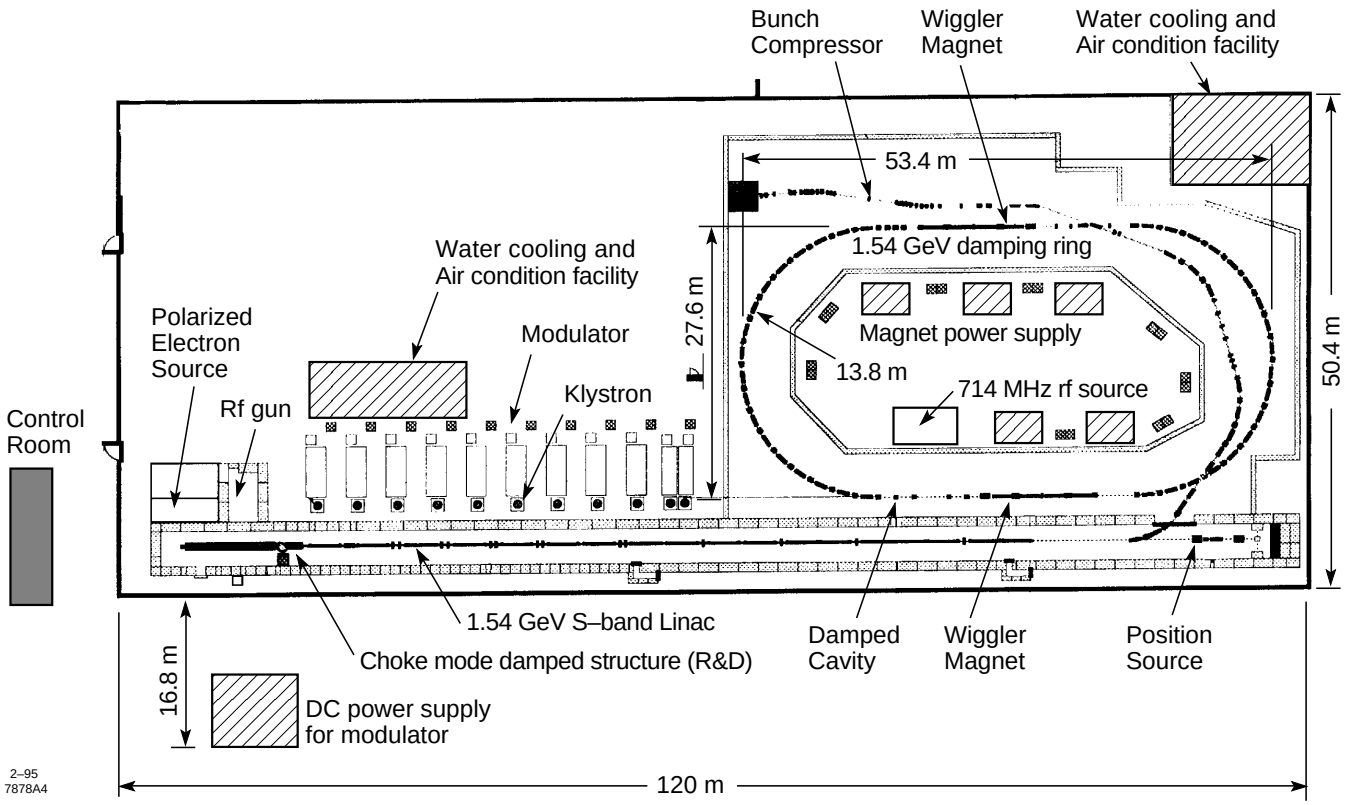

Figure 6: Layout of the ATF at KEK.

difficult. Moreover, it is beyond the present technology to measure the quadrupole and higher order fields of such a long magnet with a sufficient accuracy.

Collision Point. It is essential to measure the position and profile of incoming bunches. The vertical dimension σ_y is as small as several nanometers. A laser-compton profile monitor was developed and successfully tested at the FFTB line for beam sizes of several tens of nanometers by using 1.06 mm laser beams. For the JLC, this scheme depends critically on the feasibility of intense laser beams of one tenth of the wave length.

The background problem is another serious issue at the collision point. Pair creation due to strong electromagnetic fields of the colliding bunches is a major cause of the background. The creation process is being analyzed in detail by use of a newly developed code, ABEL. In order to cope with noise particles, the solenoid field of the detector may be higher than 2 T. A shield must be designed to confine this field within the detector.

3.4.5 Status of the ATF Construction

Shield walls for both the injection linac and the test ring were completed in 1993. Radiation safety systems were also completed. Construction of high-power AC lines and cooling water pipings for the ring was completed by the end of 1994. (See Fig. 6.)

The 1.54 GeV S-band Linac. The first 3-m section of the linac has been in commission since August 1993. Various beam monitors have been tested with the beams. A choke cavity structure also will be tested in a few months. In parallel with the commission, construction of the linac has been continued. About half of the nineteen 3-m accelerating sections have already been installed. Nine out of ten modulators have been fabricated. A sufficient number of 80 MW klystrons are in stock.

The 1.54 GeV Test Damping Ring. One unit section of the arc has been fabricated, comprised of a defocusing dipole magnet, a quadrupole, a sextupole, and steering magnets set on a common table with precision movers. A few wiggler magnets have also been fabricated. Prototype vacuum chambers are under fabrication. Cold test of a damped cavity was completed. A 50 kW, 714 MHz klystron has been successfully tested.

3.5 CLIC: The Basic Scheme, Critical Issues, and Status of Test Facilities [8]

3.5.1 The Basic Scheme

CERN is studying the feasibility of building a 0.5–2.0 TeV e^+e^- linear collider, using classical normal-conducting traveling-wave rf accelerating sections, powered by a superconducting drive linac.

The 3–5 GeV high-intensity electron drive linac runs in parallel with the main linac. The bunched drive beam is decelerated in so-called transfer structures where 30 GHz rf power is generated and fed via standard waveguide to the accelerating structures.

Periodic replacement of the energy lost by the beam to the transfer structures is made by short sections of 6 MV/m superconducting cavities driven by 350 MHz 1 MW klystrons. The superconducting cavities and klystrons already developed by CERN for LEP are ideal for this application. Generation of the rf power by a drive linac, rather than by thousands of individual klystrons, is a distinctive feature of the CLIC design and results in a particularly simple tunnel cross section.

An obvious design aim is to make the linacs as short as possible to keep the cost down. This implies high accelerating gradients, which would normally result in a higher power requirement, but is compensated for by operating at a high frequency to maximize the rf-to-beam power conversion efficiency. CLIC has chosen to work at 80 MV/m and 30 GHz. At this frequency, wakefield effects, alignment tolerances, and fabrication problems seem just manageable, but demand state-of-the-art technology.

For a 2 TeV center-of-mass collider, each of the high-energy linacs is made up of 45,750 30-cm-long iris-loaded traveling wave sections. A relatively large aperture-to-wavelength ratio of 0.2 has been chosen for these sections to maintain the destructive effect of the single-bunch transverse wakefields within reasonable limits. The 35 mm outer diameter, which is machined to a precision and concentricity with the beam aperture of ± 1 μm, serves as the reference for alignment. Individual cells are pumped by four vacuum manifolds through radial holes. The unit cost of mass-producing the discs for these sections has been estimated by a recent in-depth cost-estimate study carried out by four independent firms to be about \$12 per cell.

A stringent test of the ability of CLIC–type sections to withstand high accelerating gradients was made at KEK in September 1993, when an 11.4 GHz traveling wave section built by CERN using the same special techniques developed for CLIC sections reached an average gradient of 85 MV/m after 50 hours of conditioning (the peak gradient in the first cell was 138 MV/m). The dark current level at 50 MV/m was < 1 μA.

Limiting the emittance blowup along the main linacs in the face of strong transverse wakefields is a concern, and sets tight tolerances on the transverse alignment of the components (typically 5 μm on BPM's and accelerating sections for 50 μm initial offsets of the quadrupoles). Such tolerances can only be achieved with a beam-based active alignment system and requires in particular micron resolution BPM's. Prototype BPM's based on simple E_{110} cylindrical cavities have been built and their ability to resolve such small displacements has been evaluated on the bench by exciting them with an antenna to simulate the passage of an off-axis electron bunch. The output E_{110} signal as a function of antenna position over a range of ± 1 μm clearly shows a resolution capability of $<$ 10 nm.

3.5.2 Critical Issues

Drive-beam generation. Generation of trains of short, high-charge bunches at 1 cm spacing is an essential and difficult element of the CLIC two-beam scheme. Three basic types of solution are being studied.

The first scheme creates the trains by combining the outputs of an array of pre-injector linacs of slightly different energies using a magnetic "switch-yard" system.

The second scheme uses the bunching capability of a Free Electron Maser (FEM) to produce the 1 cm bunch structure directly. The primary beam comes from an induction linac, after bunching in the FEM bunch trains are created by a 350 MHz chopper.

The third scheme generates the total required charge of 7 mC at low energy in long trains of long, widely spaced (6.8 ms), relatively low intensity bunches. These are subsequently compressed to 1 mm by two stages of conventional magnetic compression, accelerated to 3 GeV in a recirculating superconducting linac, and finally stacked in an isochronous ring having a circumference equal to the initial bunch spacing plus 1 cm to give them the correct bunch spacing.

Alignment and Emittance Blowup. Limiting emittance blowup in the main linac is a serious concern and requires the use of beam-based active alignment schemes and sophisticated alignment correction algorithms. Although results from computer simulations indicate that this is in fact feasible, it does require a measurement of the emittance at many locations along the linac. At this moment no suitable emittance measurement device is available.

Luminosity. Further studies of schemes using damped or detuned structures are required to evaluate the feasibility of running the CLIC machine in a multibunch mode to either increase the luminosity-to-power ratio or to reduce (δ) the energy-loss parameter.

3.5.3 Status of Test Facilities

CERN has built, and is currently operating, a test facility for linear collider studies (the CLIC Test Facility or CTF) to:

- study the production of short, high-charge electron bunches from laser illuminated photocathodes in rf guns,
- generate high-power 30 GHz rf pulses by passing bunch trains through transfer cavities for testing CLIC prototype components, and
- test beam position monitors.

Significant amounts of 30 GHz power can only be extracted from the CLIC section by using bunch trains. 60 MW has been generated by a 24-bunch train containing 67 nC of total charge or 2.8 nC per bunch. This power level corresponds to a decelerating field in the section of 110 MV/m (more than the CLIC nominal accelerating gradient). The charge per bunch which can be transmitted through the structure is at this moment limited by wakefields in the traveling wave accelerating section. The accelerating field in the second CLIC structure is determined from the difference between maximum and minimum energy gain of the beam as its phase with respect to the beam-induced rf accelerating field is varied. An average accelerating gradient of 73 MV/m was measured in this way for the best performance so far. Plans to increase the 30 GHz power generation include:

- raising the gradient in the accelerating section to reduce the effect of wakefields,
- making shorter bunches using a magnetic bunch compressor, and
- building a new 100 nC/bunch rf gun.

CLIC Alignment Test Facility. An active alignment test facility has been built in an unused underground tunnel at CERN to study the feasibility of making controlled submicron displacements and to try out alignment systems.

The structures to be aligned, dummy accelerating sections for the moment, are supported by V–blocks on 1.4-m-long silicon carbide girders. The ends of two adjacent girders sit on a common platform which ensures continuity of position between units.

The platforms are activated by three stepping-motor-driven precision jacks (two in the vertical plane for vertical displacement and axial rotation, and one in the horizontal plane). The setup is equipped with linear and angular displacement transducers (0.1 μm and 10 μ-rad resolution respectively) and is piloted remotely from a small computer. After deliberate misalignments of 1 mm, the system which is programmed for automatic alignment with respect to the transducers, settles back to nominal positions within < 1 μm.

The set-up is also being used to test a new optical pre-alignment system, developed by NIKHEF in Amsterdam, for use before injection of the beam. The image of a square-shaped red-light source is focused on a light-detecting four-quadrant cell by a thin lens. Displacements of the source, lens or four-quadrant cell out of the optical axis of the instrument produce an imbalance at the detector. This system has been incorporated into the six hollow support girders of the test module and enables the relative positions of the far ends of two adjacent girders to be maintained in position with respect to the ideal straight line to < 2 μm.

The CESTA Test Facility. A collaboration to study the use of an FEM to create the CLIC drive beam exists between CERN and the Centre dEtudes Scientifiques et Techniques dAquitaine (CESTA) in Bordeaux. The aim is to use a helical wiggler to bunch a beam from an induction linac, and in a later phase to use this beam to generate power in a CLIC transfer structure. A preliminary experiment to measure the bunching produced by a helical wiggler using the beam from a gun-diode is already underway.

The MIT Test Facility. CERN is collaborating with MIT to test CLIC prototype components. MIT has a gun diode driven FEL that produces 20-ns-long, 60 MW power pulses at 33 GHz. This facility is at present being used to test a 25-cell prototype CLIC accelerating section.

3.6 The S-Band Linear Collider [9]

Among the different design studies for a next generation e^+e^- linear collider, the SBLC approach follows the concept of a relatively low rf-frequency $\omega_{\rm rf}$ and a moderate accelerating gradient g. This allows for a high overall efficiency and relaxed tolerances in combination with reduced wake field effects in the linac (the wake fields scale approximately as $W_\parallel \propto \omega_{\rm rf}^2, W_\perp \propto \omega_{\rm rf}^3$). In the SBLC, conventional traveling wave accelerating structures at 3 GHz are used running at a gradient of 17 MV/m. To a certain extent the SLC can be considered a 20% model for the SBLC and thus the SBLC can greatly make use of the wealth of experience from running this first linear collider.

The SBLC linear collider study is pursued at DESY in the frame of an international collaboration with institutes in China, France, Germany, Japan, Netherlands, Russia, and USA contributing to the technical R&D and/or the design of the 500 GeV collider.

3.6.1 Parameters

The achievable luminosity of a linear collider is determined by the following basic parameters:

- average power per beam P_b, which is limited by a reasonable AC-power limit and the overall AC-to-beam transfer efficiency η,
- normalized vertical emittance ε_y, limited by tolerances, and
- maximum tolerable beamstrahlung energy loss $\langle \Delta E/E \rangle_{\rm rad}$ limited by background considerations and the energy resolution required by the high-energy physics experiment.

Using basic relations for the luminosity and the beamstrahlung, and assuming an optimum beta-function β_y at the IP equal to the bunch length σ_z the luminosity is in good approximation given by

$$L = \text{const.} \times \frac{P_B}{\gamma} \frac{\left\langle \Delta E \; E_{\rm rad}^{1/2} \right\rangle}{\varepsilon_y^{1/2}}. \qquad (6)$$

With P_B the beam power in MW, $\left\langle \Delta E \; E_{\rm rad}^{1/2} \right\rangle$ the energy loss due to beamstrahlung in percent, and ε_y the vertical emittance in 10^{-6} m, we find the const/γ $\approx 2.8 \times 10^{32}$ cm^{-2} s^{-1} at $E_{\rm c.m.} = 500$ GeV. A large efficiency is achieved by accelerating long bunch trains per linac pulse allowing for high P_B, at the same time keeping beamstrahlung at a low level. The required emittances and beam sizes at the IP are close to what has been achieved recently at the FFTB experiment. The main S–Band Linear Collider parameters are given in Table 9.

Table 9: Main Parameters of the S–band 500 GeV (c.m.) Linear Collider.

Parameter	Value
Active length	29.4 km
$t_{\rm pulse}$	2 μs
n_b/pulse	125
Δt_b	16 ns
$f_{\rm rep}$	50 Hz
$\varepsilon_x/\varepsilon_y$	$10/0.5 \times 10^6$ m
β_x^*/β_y^*	22/0.88.8 mm
σ_x^*/σ_y^*	670/28 nm
σ_z	0.5 mm
$\left\langle \Delta E E_{\rm rad}^{1/2} \right\rangle$	3.2%
P_b	2×7.2 MW
$P_{\rm AC}$ (2 L's)	113 MW
$\eta_{\rm AC-to-beam}$	13%
L (including H_D)	3.6×10^{33} cm^{-2} s^{-1}

Table 10: Results of Beam–Beam Simulations for the SBLC.

Parameter	Value
$\left\langle \Delta E E_{c.m.;rms}^{1/2} \right\rangle$	2.7%
Disr. D_x/D_y	0.4/8.5
angle $\theta_{\gamma x/y}$	1.28/0.55 mrad
$N_{\rm pair}$/bunch	7
$N_{\rm hadr}$/bunch	0.2

3.6.2 Interaction region, Final Focus, and Collimation

Keeping beamstrahlung at a low level is an essential prerequisite for acceptable background conditions and good energy resolution for the high energy physics experiment. The most important parameters concerning beam-beam effects are summarized in Table 10.

In case of the SBLC, beams have to cross at an angle ($\theta_c = 3$ mrad) in order to avoid the multibunch kink-instability. A reduction of luminosity caused by an effective increase of the horizontal beam size is avoided by employing a simple crab-crossing scheme with finite dispersion at the interaction point), making use of a coherent energy spread within the bunch of about $\sigma_E = 0.5\%$.

The lattice between the interaction region (IR) and the main linac consists of the final focus system (FFS) for beam size demagnification and chromatic corrections, a collimation section to protect the IR quadrupoles from large amplitude particles, and bending sections for creating a sufficient separation between two beam lines if the collider has to serve two experiments. The bend between collimation and the FFS also helps to reduce background due to muons originating at the collimators.

The momentum acceptance of $\pm 2.0\%$ ($\sigma_{E,r,\rm beam} = 0.5\%$) with an optimized sextupole distribution of the FFS for the SBLC design is far in excess of the beam energy spread. The requirements for beam collimation are determined by the condition that synchrotron radiation generated in the doublet before the IP has to pass freely through the aperture of the final quadrupole on the opposite side. This means that particle amplitudes have to be restricted to $6\sigma_x \times 8\sigma_y$. Following concepts developed at SLAC, a beam optics design for simultaneous collimation in x, y and dE/E has been worked out. The entire lattice from the linac to the IP will require approximately 1.1 km on either side of the IP.

3.6.3 Main Linac

As any other Linear Collider, the SBLC consists of a large number of basic cells. In the SBCL such a cell is made of two 6-m-long traveling wave, constant-gradient copper structures. They are powered by one 150 MW klystron. A modulator flat top pulse width of 2.8 μs is required to handle the current pulse of 2 μs.

A total of 2450 klystrons and modulators is necessary for the two 250 GeV linacs. Different focusing schemes are still being considered, while in general the focusing

strength should vary with $\beta \propto \gamma^{1/2}$ in order to keep the BNS energy spread constant. After the damping ring the basic FODO cell length with $\beta_{\text{initial}} = 18$ m is determined by the length of one accelerating structure. Further upstream the β–γ scaling could be realized in good approximation by distributing fewer quadrupoles of the same focal length along the linac. This scheme has the advantage of keeping the number of different units down.

In order to minimize the civil engineering costs it is planned to have the klystrons and the linac housed in one single tunnel. Preliminary radiation simulations have shown that legal restrictions can be met by employing suitable concrete shielding between the accelerator and the klystron gallery.

One of the most important accelerator physics issues in a linear collider is the preservation of a (very) small emittance along the linac. Emittance dilution caused by chromatic effects (dispersion, filamentation) due to energy spread in the bunch, short range wake fields and long range deflecting modes are investigated extensively. Recent computer simulation results for SBLC show that single bunch beam break-up due to injection oscillations can be well suppressed by applying BNS damping only over the first 30% of the linac employing a coherent energy spread of $\sigma_E = 0.9\%$. In the remaining part of the linac σ_E can be reduced again to 0.3% by shifting the bunches 12 degrees off the rf wave crest. Taking into account transverse positioning errors of quadrupoles, accelerating structures and beam position monitors (BPMs) of 0.1 mm (rms), it is shown that after applying various correction algorithms (wakefield-free (WF) orbit correction, bumps for dispersion and wakefield compensation), the dilution can be kept as small as $\Delta\varepsilon_x/\varepsilon_y = 3\%$. For a BPM resolution of 5 μm this correction scheme requires four emittance measurement stations with an accuracy of 3%.

Higher order modes, induced by bunches passing off-axis through the accelerating structures, cause oscillations growing over the entire bunch train and along the linac (cumulative multibunch beam break-up). In order to keep this effect within limits, a frequency spread for the deflecting modes is introduced (the maximum variation is assumed to be 40 MHz) by changing the resonant behavior of the rf structure for the HOM modes and at the same time keeping it identical for the accelerating mode. Since detuning alone is not sufficient, the quality factor of the modes with the strongest coupling to the beam have to be lowered. This is achieved by adding three HOM-couplers per structure resulting in a Q-profile of typically $\approx 3 \times 10^3$ for the harmful dipole modes. With these assumptions and tolerances, computer simulations yield an effective multibunch emittance dilution of $\Delta\varepsilon_x/\varepsilon_y = 20\%$. This dilution can be further reduced by "beam-based alignment" of the cavities (zeroing of the HOM power by moving the structures towards the beam axis) and/or by using fast kickers to place all bunches back on the same orbit from pulse to pulse. The latter method requires pulse to pulse stability of the beam break up behavior.

3.6.4 Injection

The emittances required for the SBLC beams are provided by two damping rings of 650 m circumference operating at 3.15 GeV. A beam optics delivering $\varepsilon_x = 5 \times 10^{-6}$ m (50% of the design value at the IP) has been designed. The normalized dynamic aperture of 2.4×10^{-2} m is sufficient to accept the beam delivered from the e^+ source. Positrons are produced by converting γs in a thin ($0.4x_0$) target. The required intense photon source is realized by passing the e^- beam after collision through a 30-m-long wiggler. This method drastically reduces the heat load on the target and opens up the possibility to produce polarized positrons by using a helical undulator.

3.6.5 Upgrade Potential

The SBLC design is very well suited for pushing the vertical emittance to lower values in a later upgrade program. After gaining experience with various correction and optimization procedures, reducing the vertical emittance ε_y by an order of magnitude seems to be conceivable. This reduction would allow for higher luminosity and at the same time lower AC–power consumption. Achieving such small emittances becomes very important (if not inevitable) for an energy upgrade to 1 TeV. In the SBLC design such an upgrade could be realized without extending the overall tunnel length. It would require doubling the number of klystrons and compressing the rf-pulse with a SLED system. Both means together provide the accelerating gradient of 34 MV/m needed to reach 1 TeV within the existing linac length. The price to pay though is a doubled overall power consumption.

3.6.6 Test Facilities

The goal of the SBLC test facility under construction at DESY is to construct and test the basic components required for the 2×250 GeV linear accelerators. The test linac consists of an injector providing bunch trains similar to those to be used in the collider. Two 150 MW klystrons (built by SLAC) power four 6-m-long accelerating structures. A beam diagnostics station is foreseen to measure bunch to bunch offsets as well as single and multibunch energy-spread. The injector provides a 6 A pulse out of a 90 kV gun with a duration of 2 ns. This pulse is compressed longitudinally by more than a factor of 200 resulting in a bunch length

of $\approx$ 3 mm. Although longer than the final design bunch length, this value is sufficient to study most multibunch and beam dynamics effects. The subharmonic cavities and the vacuum system will be assembled and installed during 1994 and be commissioned early 1995.

Recently, the first klystron has reached its full design parameters in rf tests at SLAC. Conventional line-type modulators are foreseen for pulsing the klystrons. As an alternative solution a hard tube switching device is also under study at DESY. A klystron test stand for the 150 MW klystron with water loads and further required infrastructure is under construction.

The design of the accelerating sections concentrates on the first series production of 5.2-m-long structures for the DESY injector linac, which are very similar to the test facility structures. Nine-hundred cells for 6 sections (from overall 14) have been ordered from industry and are being brazed at DESY. Horizontal or vertical brazing, vacuum- or hydrogen-atmosphere ovens or inductive heating are still being investigated. A cup-tuning machine to match the structure for the accelerating wave after brazing and before final installation is now operating.

Low power test models of the symmetric high-power couplers have been manufactured and matched to an accelerating structure while the high power versions are scheduled autumn 1994. Different types of additional couplers required for the HOM damping and/or measurement of the beam induced higher order mode power are being investigated. After brazing and tuning, the sections for the test facility will be mounted on different types of temperature insensitive girders (glass ceramics, carbon fiber composite and heat shielded stainless steel) to keep the six meters of copper waveguide straight within 15 μm rms. Every girder is equipped with micromovers at both ends to allow for $\pm$1.5 mm offset in both directions.

Magnets, structure supports, and precision movers, as well as methods to compensate ground vibrations, are investigated. The design of the linac quadrupoles completely decouples the coil windings from the iron yoke, which automatically minimizes the vibration effects due to cooling water flow. Although the effects which have been described before will not affect the final emittance in the test accelerator, feedback systems and control loops will be tested on the supports and girders, which have been designed to fit the tunnel requirements and the minimum height for final installation.

3.6.7 CONCLUSION

The low-frequency approach of SBLC is well suited to achieve the performance goals of a next generation linear collider based on extensions of available technology. At the same time, it is also well suited for later upgrade programs to either higher luminosity or higher energy without enlarging the overall size of the machine.

3.7 TESLA: The Superconducting Radio Frequency Approach[10,11]:

3.7.1 The Basic Approach

All electron-positron linear collider designs are constrained by the need to limit the number of photons emitted during each beam-beam interaction. The practical result of this is that the luminosity is simply proportional to the ratio of the beam power to the beam area at the crossing point.

$$L = \text{const} \cdot [\mathrm{P_{beam}}/\mathrm{Area}] \qquad (7)$$

The constant is determined by the number of photons deemed acceptable in a particular design. Copper-based designs need to minimize the required beam power by working with the smallest feasible beam cross section area. In this case, the AC power is naturally large because of the significant I^2R losses required to establish the accelerating gradient and the relatively low efficiency in converting mains power to beam power. There is also a premium in using as high a frequency as possible since that reduces the wall loss for a given accelerating gradient. At higher frequency, the conductors are closer to the beam making tolerances tighter and the emittance diluting wake effects stronger.

This situation is radically altered if the accelerating cavity walls are superconducting. In this case the wall losses are reduced by several times 10^5 and the efficiency of conversion of mains power to beam power can be relatively high, with the added dividend that conventional rf power supplies can be used. The low loss permits use of a lower frequency for the superconducting version with small power penalty, thereby ameliorating the wake effects. Further, because of the higher relative efficiency, it is possible to use more of a given, total, facility power in the beam, thereby allowing use of a relatively larger beam area at the crossing. A concomitant of the low wall losses and relatively large beam area is the ability to deliver the beam in long pulses with bunches separated on the order of a microsecond in headon collisions, with relatively long free space on either side of the IP, $L*$ being of the order of 3 m.

The needed emittances are achievable with damping rings in existence today and the demagnification required of the final focus has already been demonstrated at the FFTB experiment at SLAC. It should be noted that even in the TESLA case, the beam cross section at the crossing point will be smaller than in present practice at the SLC and of greatly reduced aspect ratio. A proposed layout for TESLA is shown in Fig. 7.

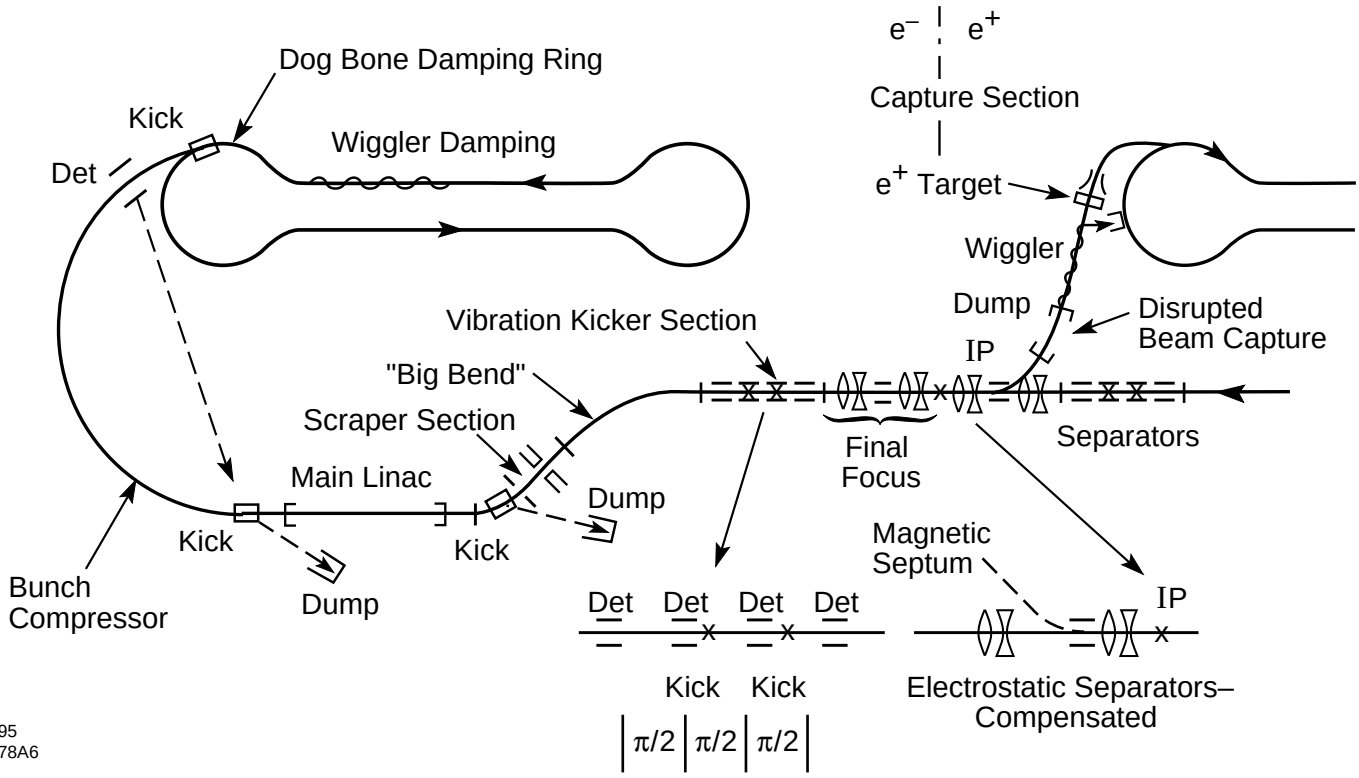

Figure 7: Shown is an example of a positron damping ring and a collision region that takes advantage of the long pulses and microsecond separation to give head-on collisions with an in-pulse feedback on bunch position and compensated electrostatic separation of the beams after the collision.

3.7.2 Critical Issues

While the potential advantages are manifest, technical realization will be challenging. There are both cost and technical factors to be considered. On the cost side the achievable gradients need to be raised from the 5 MeV/m typical of existing storage ring cavities to 20 or 25 MeV/m. The cost per unit length of the accelerating cavity plus cryostat needs to be lowered a factor of five to bring the price to about 50k$/m to give a competitive cost per MeV figure. Another source of concern is the relative delicacy of the superconducting state. How reliable would such a system be in the face of the realities of vacuum and cryo system failures? Will it be possible to recover from such a failure by in situ processing? At the long rf wavelength, which is a strength of the SC approach, electrons present in the accelerator vacuum can be more easily captured from rest to make parasitic beams. These parasite beams could perhaps sap energy from the main beam and perhaps cause unwanted cryo losses and beam background in addition to instabilities of the wanted beam. Because of the very high Q of the cavities, small changes in dimension can make large changes in amplitude and phase of the accelerating wave. The pressure caused by the growing stored energy during the pulse can make such changes, the so-called Lorentz detuning. Can an economical cavity stiffening with active control scheme be found? Finally, the large beam power which is on the one hand a virtue implies the need for the most powerful positron source of all the approaches and gives the challenge of safe disposal of the high beam power in addition. Progress in all of these areas has been made and a plan to demonstrate solutions to many of them put in place.

3.7.3 Progress of the TESLA Test Facility

A 500 MeV TESLA Test Facility Linac (TTFL) is now under construction at DESY. It will consist of four cryomodules of a type that could be used in a linear collider. Each module contains eight 1 m, nine-cell cavity units, plus a focusing doublet assembly with beam monitors. Each cavity subunit has its own couplers. Two cryomodules are driven by one klystron/modulator set. An injector section brings the initial beam up to 15 MeV nominal before introduction into the TTFL proper. A beam analysis station will be installed both after the injector and at the high-energy end of the TTFL. The linac will be installed in Halle 3 at DESY adjacent to the recently completed cavity chemical processing area,

with cleanrooms, vertical test cryostats, and rf power supply for cavity testing and high-power pulse processing (HPP). The cavities and the cryostat have been ordered for the first cryomodule, with delivery expected in early 1995. Initial cavity tests have begun. In a prototype processing and test setup at Cornell, several multicell cavities have been chemically processed and subjected to HPP.

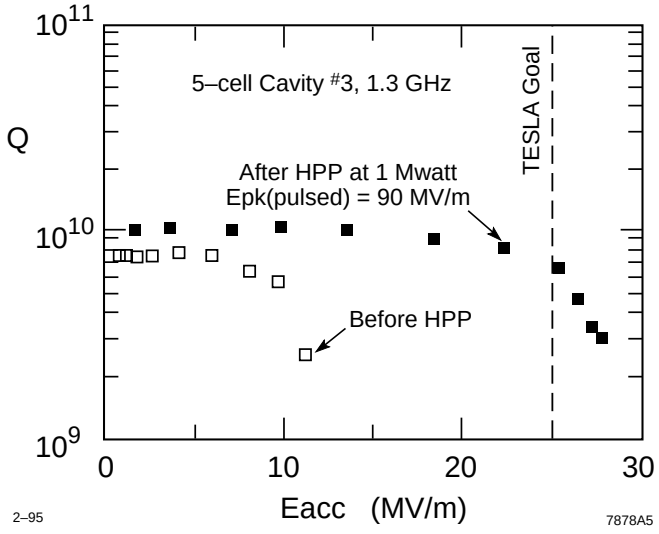

Figure 8: Q versus accelerating field before and after HPP.

Figure 8 shows the Q versus Field, CW, before and after HPP. It can seen that HPP is quite effective in raising the achievable gradient. After exposure to air, HPP was successful in recovering the gradient. How this will apply in a linac environment must await the completion and operation of the TTFL now expected in the 1997–1998 time frame. Experience with the facility will yield information about many of the critical issues cited above; for example, dark current, Lorentz detuning, cost, robustness against vacuum or cryogenic failures, and so on.

3.8 Results from the Final Focus Test Beam (FFTB) [12]

One of the challenges to the development of TeV-scale e^+e^- linear colliders is to make particle beams with extremely small sizes. Whereas the bunches in the SLC are millimeter-long needles a micron across, those in future machines will need to be ten times shorter and up to a hundred times narrower. Producing and colliding tightly focused beams requires careful control and stabilization of magnetic elements, and places considerable emphasis on accurate measurement of the properties of the beam itself. The FFTB Collaboration [13] has completed construction of a prototype focussing system for a future linear collider (see Fig. 9). This FFTB, which occupies 200 m in the straight-ahead channel at the end of the SLAC linac, is designed to accept the SLC electron beam as input and to produce a focal point at which the beam height is demagnified by a factor of 380, to a size smaller than 100 nm. Similar compression factors will be required for the final focus of TeV-scale linear colliders.

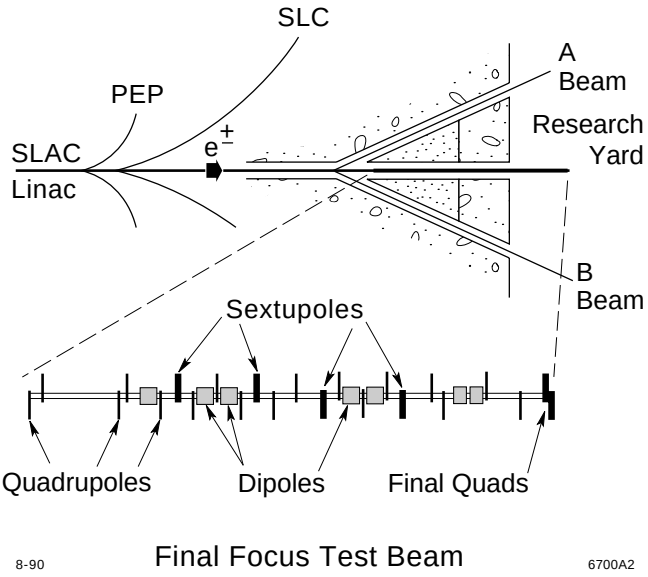

Figure 9: Location of the FFTB at the end of the SLAC 50 GeV inac.

Results presented here were obtained with 0.65×10^{10} electrons per pulse transported to the end of the linac with a vertical emittance of typically 2×10^{-6} rad m.

The nominal beam energy was 46.6 GeV, and the spread in particle energies was maintained at $\pm0.05 - -0.1\%$. The optics of the FFTB are corrected to third order for geometric and chromatic aberrations, and are designed to reduce this beam to a spot with vertical height of 52 nm.

The FFTB contains five optical sections. The beam at the end of the linac is first matched to the lattice of the FFTB in a section that controls the launch of the beam into the FFTB, and contains quadrupole lenses, both normal and rolled, that are able to fully adjust the betatron space of the beam. Two sections that contain sextupole magnets at points of high dispersion allow the chromaticity of the lattice to be tuned separately in the horizontal and vertical planes. The chromaticity introduced by the focussing quadrupoles must be cancelled with approximately 1% accuracy by that generated in the sextupoles. Geometric aberrations are controlled with pairs of sextupoles placed at points of equal dispersion but spaced exactly π radians apart in betatron space. These aberrations must also be

cancelled to $\approx$ 1%, so it is important to maintain the proper phase advance between the sextupole magnets. The lattice includes a "β–exchanger" to match the optics from one chromatic correction section to the other. This section contains an intermediate focal point at which the vertical beam height is reduced to 1 μm. The overall demagnification of the beam is determined by the focal lengths of the initial matching section and the final telescopic section. The basic principles of this scheme have been successfully demonstrated at the SLC, but the demagnification of the beam in the FFTB is an order of magnitude greater.

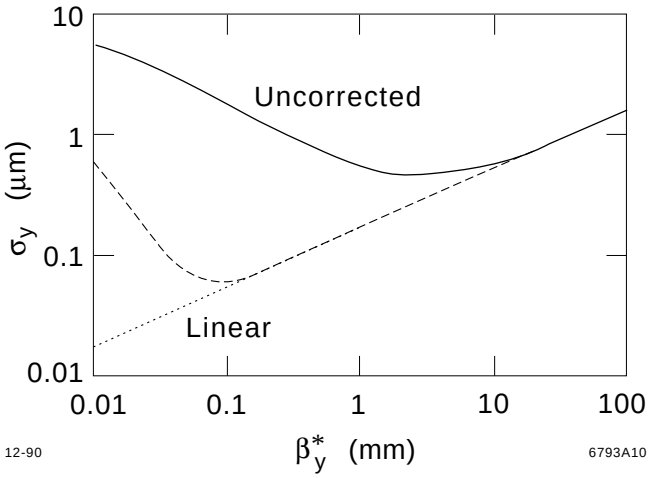

Figure 10: Vertical beam height at the FFTB focal point. The curves are uncorrected for chromaticity (solid), corrected for chromaticity (dashed), and the ideal monochromatic behaviour (dotted).

Two major third-order aberrations remain in the spot produced by the FFTB. Geometric aberrations are introduced as the beam envelope changes within the finite length of the sextupoles. Also, synchrotron radiation in the bend magnets destroys the exact cancellation between the chromaticity introduced by the sextupoles and that by the quadrupole lenses. An optimal design that minimizes the spot dilution from these two effects is used. Its performance is shown in Fig. 10. A similar optimization that includes the emittance growth due to synchrotron radiation in the bend magnets is done for the horizontal plane.

The optical design is tailored so that 28 of the 31 quadrupoles required to focus the beam are constructed as identical solid iron-core magnets each with an effective length of 46 cm and bore diameter of 2.3 cm operated with pole-tip fields below 10 kG. The design of the pole-tip contour limits the non-quadrupole field to less than 0.1% of the primary field at 70% of the full aperture. Tolerances on the lenses of the final doublet are more stringent with restriction on their harmonic content of 0.03%, and in some cases these magnets must operate with pole-tip fields as large as 14 kG. Permendur is used in the fabrication of the pole-tips of these magnets. There are four sextupole magnets in the chromatic correction sections of the FFTB. The field in each need only be pure to 1%. All FFTB magnets meet or exceed the requirements for strength and harmonic content.

Errors in the position or orientation of magnetic elements in the FFTB (with respect to the ideal beam line coordinates) can introduce anomalous dispersion or coupling into the beam phase space and can change the focusing of the optics. Alignment errors also introduce linkage between the correcting elements of the beamline.

Optical effects created by errors in the alignment of the main FFTB magnets can be corrected with vernier tuning elements as long as the alignment is within certain tolerances. Simulations showed that spot sizes could be created at the focal point that differ from the design value by only several percent, as long as the magnetic centers of the quadrupole and sextupole magnets are initially placed within 100 μm of their ideal horizontal and 60 μm of their ideal vertical positions.

Each quadrupole and sextupole magnet in the beamline is placed on a remotely-controllable support capable of translating laterally over a range of 1 mm in steps of 0.3 μm. The design uses a set of cam shafts driven by precision stepping motors. Shown in Fig. 11 is the response of a typical magnet mover. These devices are linear to a few parts per mil over their full range of motion, and are able to move quarter-ton magnets with submicron precision and little or no backlash. The precision of these movers makes it possible to use the beam to accurately align the FFTB magnets, and to simultaneously calibrate the response of the beam position monitors. Magnet-to-magnet alignments of 10–50 μm are estimated to be achieved with application of beam-based procedures.

Carbon filaments used in wirescanners are destroyed by thermomechanical stresses induced by submicron beams, so new instrumentation is required to measure beam profiles at the final focal point of the FFTB. Two devices were built for this purpose. One monitor uses the coherent interaction of the electron bunch with a gas-jet. Atoms of helium or argon, injected into the path of the beam, are ionized and trapped in the potential-well created by the passing electron bunch. Plasma oscillations, excited in the plane transverse to the beam direction, effectively transfer energy to the ions. The amplitude of the oscillations in the horizontal and transverse planes are proportional to the corresponding dimension of the electron bunch, so the azimuthal distribution of ejected ions reflects the aspect ratio of the bunch. The distribution and time-of-flight of the ejected ions are detected in a ring of multichannel plates that surrounds the focal point.

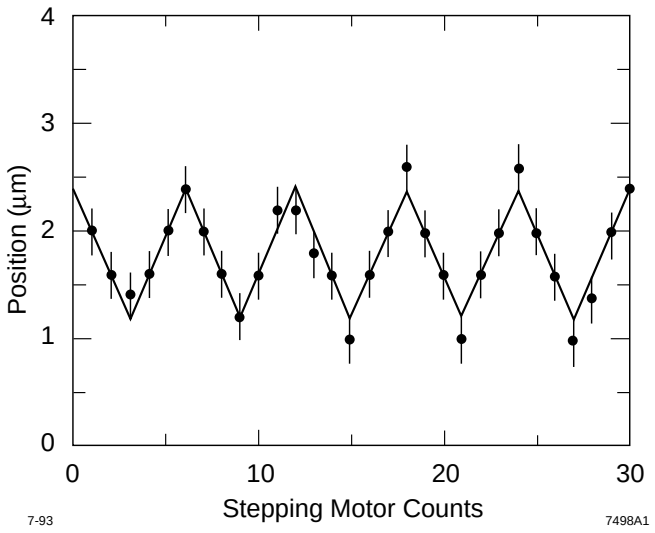

Figure 11: Measured response of a magnet mover. The solid line traces the input command value, and the points are the measured response of the mover. The errors on the points are the estimated resolution of the position readout.

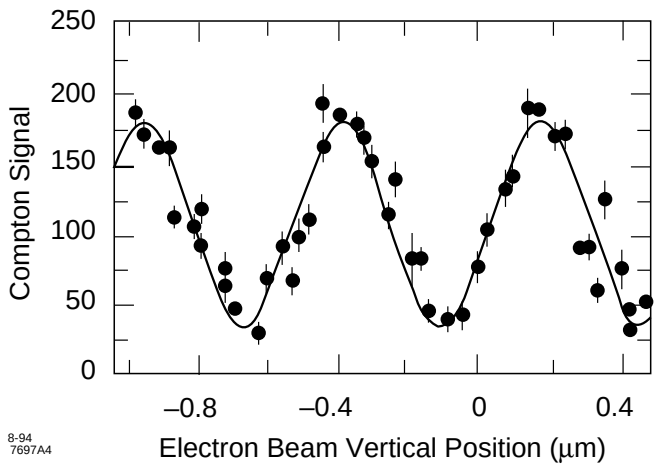

Figure 12: Measurement of the vertical height of the beam at the FFTB focal point with the laser-Compton spot monitor. Observed fringe spacing agrees well with the 0.5 μm expected from the wavelength of the laser. In this case, the beam height is 73 nm.

A second monitor built for the FFTB focal point uses the concept of an optical cavity. A laser beam is split, and folded onto itself to produce an interference fringe pattern in space. The electron beam is scanned across this pattern to yield a modulated rate of Compton-scattered photons in the forward direction. The ratio of peak to minimum Compton rates depends on the size of the beam and the fringe spacing.

Time-of-flight signals and azimuthal distributions from the gas-jet monitor agreed well with theoretical expectations, and were used to optimize the position of the beam waist, and to adjust skew quadrupoles to remove astigmatic coupling introduced by the final quadrupole lenses. This monitor was able to measure beam heights from a few microns down to 100–200 nm, and was an important tool to make intial adjustments of the beamline optics.

Precise tuning of the smallest spots was achieved with the laser-Compton monitor. Iterative tuning of vernier knobs to minimize residual dispersion and coupling of the beam phase space resulted in beam heights $\sigma_y \approx 100$ nm. Further reduction was made by adjustment of trim sextupoles just upstream and at the same betatron phase as the final quadrupoles. An example of the measurement is shown in Fig. 12. The beam size measured by the laser-Compton monitor must be corrected for the mismatch between the length of the electron bunch, its divergence at the focal point, and the extent of the laser field along the beamline. This is estimated to be a 10% correction. Repeated measurements taken at the focal point over a period of several hours were distributed approximately Gaussian with corrected mean 70 nm and standard deviation 6 nm.

We conclude that we have focused the SLC 47 GeV electron beam through a demagnification $\approx$ 320 to a vertical height of $\sigma_y \approx 70$ nm. This represents a significant advance of technologies and accelerator physics required for the design and implementation of a future TeV-scale electron-positron collider.

3.9 The Next Linear Collider Test Accelerator [14]

3.9.1 Introduction

During the past several years, there has been tremendous progress on the development of the radio frequency (rf) system and accelerating structures for a Next Linear Collider (NLC). Developments include high-power klystrons, rf pulse compression systems and damped/detuned accelerator structures to reduce wakefields. In order to integrate these separate development efforts into an X–band accelerator capable of accelerating the electron beams necessary for an NLC, SLAC is building an NLC Test Accelerator (NLCTA). The goal of the NLCTA is to bring together all elements of the entire accelerating system by constructing and reliably operating an engineered model of a high-gradient linac suitable for the NLC. The NLCTA will serve as a test-bed as the design of the NLC evolves. In addition to testing the rf acceleration system, the NLCTA is designed to address many questions related to the dynamics of the beam during acceleration. In this section, we will report on the status of the design, component development, and construction of the NLC Test Accelerator.

Table 11: NLCTA rf System Parameters.

Parameter	Design	Upgrade
Linac unloaded energy gain	540 MeV	1080 MeV
Linac active length	10.8 m	10.8 m
Unloaded accelerating gradient	50 MV/m	100 MV/m
Injection energy	90 MeV	90 MeV
rf frequency	11.424 GHz	11.424 GHz
Number of klystrons	3	6
Klystron peakpower	50 MW	100 MW
Klystron pulselength	1.5 μs	1.5 μs
rf pulse compression power gain	4.0	4.0
Phase advance/cell	2 π/3	2 π
HOM suppression technique	Detuning	Detuning

In order to control the linac length of the NLC, current designs at SLAC and KEK use acceleration gradients which begin at 50 MV/m for the 0.5 TeV linear collider and finish with 100 MV/m in the upgraded 1 TeV or 1.5 TeV collider. These gradients are provided by an 11.4 GHz rf system (X-band). Although there has been experience with short X–band accelerators in industrial and medical applications, there are presently no high-gradient X–band accelerators in operation.

Much experience has been gained during the past several years with this radio frequency at SLAC and KEK. We have powered 11.4 GHz structures to reach peak surface fields in excess of 500 MV/m. Short traveling-wave accelerating structures have been powered to accelerating fields in excess of 100 MV/m. High-power klystrons have been constructed which reach 50 MW in pulses 1.5 μs long and 85 MW in pulses 200 ns long. We have constructed high-power rf pulse-compression systems that achieve a factor of four to five in peak-power multiplication. More efficient modulators are being developed. Finally, we are developing low-loss components for manipulation of high-power pulses of 11.4 GHz rf.

The NLCTA is primarily a high-gradient X-band linac consisting of six l.8 m-long accelerator sections. These sections are fed by three 50 MW klystrons, which make use of SLED–II pulse compression to increase the peak power by a factor of four. This yields an acceleration gradient of 50 MV/m, so that the total unloaded energy gain of the beam in the X–band linac is 540 MeV. The NLCTA parameters are listed in Table 11. The right-hand column of Table 11 lists the parameters for an upgrade of the X–band linac to 100 MV/m by the use of six 100 MW klystrons.

3.9.2 Injector

The NLCTA injector will consist of a 150 kV gridded thermionic cathode gun, an X–band prebuncher, a capture section with solenoid focusing, and a rectangular chicane magnetic bunch compressor.

3.9.3 Radio Frequency System

The high-gradient accelerator will be fed with rf power through overmoded circular waveguides which penetrate the shielding blocks above the accelerator. Four 50-MW klystrons will be positioned along the accelerator, outside the shielded enclosure. Each klystron is powered by an independent modulator, allowing the flexibility needed for multibunch energy control and adequate power for an upgrade to a 100-MV/m accelerating gradient with six 100-MW klystrons, as indicated in Table 11. Each klystron feeds a SLED–II pulse compressor. The pairs of delay lines of the SLED–II pulse compressors are overlapped, parallel to the accelerator, outside the shielding. The output of each SLED–II is split to feed two accelerator sections. In the case of the injector, the SLED–II output is split to feed the two short injector sections to provide overhead for beam loading. The first two klystrons have exceeded NLCTA specifications (50 MW, 1.5 μs), and one is being used to test a complete NLCTA pulse compression system.

3.9.4 Accelerator Structure

To increase the luminosity of an NLC well beyond the minimum levels necessary for high-energy physics experiments, a train of bunches must be accelerated on each rf pulse. The primary impact of this choice is in the design of the rf structure. As each bunch traverses the structure, it excites wakefields which can remain until the next bunch passes. If this happens, each bunch resonantly drives all the bunches behind it. This leads to transverse multibunch beam breakup. However, beam breakup can be eliminated by choosing an rf structure in which the wakefields damp significantly between bunches.

There are two methods that can be used to achieve this damping. In the first, the higher order modes in the structure can be damped by coupling them to radial waveguides that are terminated with matched loads. This causes the energy to radiate out of the structure between bunches. The second technique involves changing the frequency of the higher order modes (HOMs) of each cell. Qualitatively, the total wakefield is then composed of a sum of wakefields, one from each cell. Behind the driving bunch, the wakefield decoheres because of the differing frequencies, and the net effect is a reduction of the wakefield. With this technique, the frequency distribution is important in

determining the subsequent decay of the wakefield behind the driving bunch. Both of these techniques have been tested experimentally.

For the NLCTA, we plan to use a detuned structure which is a 2/3 "constant-gradient-like" structure modified every half meter to include four symmetric pumping holes. These holes lead to parallel vacuum manifolds, which provide sufficient pumping speed despite the small beam aperture. The cavities are machined to provide a precise mechanical reference from the inside dimensions to the exterior of the structure.

In order to achieve the reduced wakefield, the structure is configured to be very nearly constant gradient. The decoherence of the wakefield between bunches will be achieved by a Gaussian distribution of HOM frequencies with a standard deviation of 2.5%, which results in a Gaussian decay in time for the initial wakefield. This distribution can be obtained by tailoring a constant-gradient section so that more cells are near the central frequency, while fewer are near the ends of the frequency band. This choice results in a structure in which the iris size along the structure first decreases rather quickly, then decreases slowly in the middle, and finally decreases quickly along the structure towards the output end.

With this distribution of HOMs, the wakefield decoheres to less than 1% of its peak value. This decoherence is sufficient to eliminate beam breakup in the NLC or NLCTA. Because of the low injection energy, the NLCTA has a sensitivity to transverse wakefields comparable to the much longer NLC linac. The NLCTA will permit the verification that detuned structures can indeed suppress wakefields to the levels necessary for stable acceleration.

The first detuned accelerator structure has been completed and tested successfully at high gradient. In addition, the resulting wakefield was measured in ASSET in the SLC and was found to agree quite well with theoretical predictions. The second structure plus the two injector structures are presently in fabrication.

3.9.5 Beam Analysis

A magnetic spectrometer has been designed that will analyze the bunch train after acceleration in the linac in order to determine beam energy, beam-energy spread, and bunch-to-bunch offsets. The optics in the beam analysis region allow for the measurement of emittance in both transverse planes. A vertical kicker magnet upstream of the spectrometer provides a method for separating the bunches vertically so that the energy, energy-spread, and horizontal offsets can be independently measured along the bunch train. After initial commissioning, an extensive set of experiments is planned to verify that the NLCTA can indeed stably accelerate trains of low-emittance bunches suitable for a full-scale NLC.

3.9.6 Summary and Plans

The NLCTA is proceeding on schedule. The accelerator shielded enclosure is complete and all infrastructure is in place (girders, cable trays, water, lights, racks, and control room). All the magnets are complete and installed in the enclosure, power supplies are installed. The prototypes for the klystron and accelerator structure have performed at NLCTA specifications. Additional klystrons and structures are in fabrication. The prototype of the pulse compression system has been tested up to full power. The injector will be tested in the summer of 1995, and the full NLCTA should be complete by end of 1996.

3.10 Summary

The Electron Linear collider Facilities section gives a snap shot of the designs for a future e^+e^- linear collider. The detailed designs are developing very rapidly as the various test facilities are being constructed. Most designs and test facilities will reach completion around the end of 1996. In order to facilitate communication and cooperation in the above process, a Linear Collider World Collaboration has recently been established. The following is an excerpt from the Memorandum of Understanding:

3.10.1 Purpose and Guidelines

This Memorandum of Understanding (MoU) describes the Collaboration formed by the Signatory Institutions for the following purpose:

- to coordinate international Research and Development (R&D) efforts towards linear colliders,
- to review and monitor the status and progress of technical approaches towards linear colliders, and
- to facilitate the exchange of personnel among the participating Institutions, and to promote the sharing of research facilities among the Participating Institutions.

This Collaboration will carry out its business according to the following guiding principles:

- The Collaboration is open to any Institution which agrees to make significant Contributions toward the development of linear colliders.
- This Collaboration is not intended to displace or supersede any existing organization.
- The Collaboration recognizes the requirement that R&D towards future linear colliders be conducted without prejudice to potential sites of construction.

- The Collaboration anticipates that future linear colliders will be constructed by international coalitions.

The Linear Collider World Collaboration is now in the process of conducting its first technical review of linear colliders. The following is the charge to the Technical Review Committee:

> *Charge to the 1994/1995 Technical Review Committee*
>
> The Technical Review Committee is to consider the goal to design, build, and operate a TeV-scale linear electron-positron collider capable of satisfying the need to explore the particle physics of this energy range. Specifically the Committee is to examine accelerator designs and technologies suitable for a collider that will initially have center of mass energy of 500 GeV and luminosity in excess of 10^{33} cm^{-2} s^{-1} and be built so that it can be expanded in energy and luminosity to reach 1 TeV center of mass energy with luminosity 10^{34} cm^{-2} s^{-1} The Committee should consider construction and operation of both the initial facility and the upgrade path to 1 TeV. The Committee is also asked to comment on the potential of technologies to reach higher energies and luminosities, and to provide alternative physics capabilities, for example gamma-gamma collision.
>
> The Technical Review Committee is to identify the accelerator physics issues and technological requirements for each approach to provide particle physics opportunities at the energy and luminosity goals stated above. The report of the Committee should contain a brief summary of the status of and expected progress toward understanding and achieving the most important of these requirements. The Committee should attempt to identify areas of possible further collaboration in the world-wide linear collider R&D program.
>
> A draft of the Committee report should be submitted to the Collaboration Council shortly after the LC95 meeting scheduled for March 1995 in Japan.

We note that the Technical Review Committee is beginning its work now and will have a draft report around the time that the Proceedings of this Workshop is published. We anticipate their report will give a more detailed and indepth assessment of the status of the world linear collider effort.

4 Electron–Positron Circular Collider Facilities

4.1 Operating Colliders and Future Plans

Currently, there are five e^+e^- circular colliders (VEPP–2M at the Budker Institute in Novosibirsk, Russia, BEPC at the Institute of High Energy Physics in Beijing, CESR at Cornell University in Ithaca, New York, TRISTAN at KEK in Tsukuba, Japan and LEP at CERN in Geneva, Switzerland) operating in the world. The total center-of-mass energy for the beams in these colliders ranges from the ϕ mass (1.020 GeV) to the Z mass (91.2 GeV). For circular colliders, the emphasis is on luminosity and on providing a very clean background environment for the detectors. Upgrade plans for VEPP–2M, BEPC, and CESR are to increase their luminosities while the operating energy of LEP will be increased to above W^+W^- threshold by the installation of approximately 200 multicell superconducting rf accelerating cavities. The luminosity of LEP will also be increased by a more aggressive pursuit of multibunch operation with pretzels with initial operation planned for 1996.

Future plans are for the completion of the construction of PEP II, a B Factory at SLAC in Stanford, California and KEK B, a B Factory at KEK. Both machines are being constructed in existing tunnels at these laboratories and will operate with asymmetric beam energies to provide a significant Lorentz boost for the center of mass in the laboratory frame. This makes it possible to observe the time evolution of the B^0 decays from the $\Upsilon(4S)$ and thereby the violation of CP for the first time outside the K system. At Frascati in Italy, a ϕ Factory, DaΦne is under construction with initial operation expected in early 1996. At Cornell, CESR's luminosity is being increased to the region of $10^{33}\,\mathrm{cm}^{-2}\,\mathrm{s}^{-1}$ to provide a large data sample at the $\Upsilon(4S)$ for the study of rare B decays in an upgraded CLEO detector. The remainder of this short chapter will be a small expansion of these remarks on each of the colliders.

4.2 Facilities

4.2.1 Phi Factories

VEPP–2M at the Budker Institute in Novosibirsk has been operating for the past several years with a peak luminosity of 5×10^{30} cm^{-2} s^{-1} and currently has the highest luminosity of any collider in this energy region. An upgrade in luminosity is planned for the end of 1995 by installing a solenoidal final focusing system. This will permit operation with round beams and has the potential of increasing the luminosity by a factor of 20. It will be the first extended operation of round beams in a circular e^+e^- collider.

Table 12: DaΦne Main Features.

Initial luminosity	1.3×10^{32} cm $^{-2}$ s^{-1}
Luminosity in 3 years	$\times3$ increase
Interaction regions	KLO, CP violation
	FINUDA, hypernuclei
Circumference	97.69 m
Bunches	initial: 30, final:120
Particles/bunch	8.9×10^{10}
Radio frequency	368.25 MHz
Cavity design, single cell	Low HOM impedance
Feedback	DSP-based longitudinal similar to PEP II
Initial operation	Early 1996

DaΦne is being constructed at Frascati in buildings previously occupied by ADONE, one of the first successful modern e^+e^- colliders, which was retired in April 1992. The main features of DaΦne are listed in Table 12.

4.2.2 Tau Charm Factories

The collider at the High-Energy Institute in Beijing, BEPC continues to be the premier facility in this energy region. An upgrade of the luminosity of the collider is planned and an improvement program for the detector is currently underway. The projected peak luminosity performance is 3×10^{31} cm^{-2} s^{-1}, which will be an increase of approximately a factor of 5 over present peak performance.

A project to construct a high-luminosity collider in Spain by a consortium of European and US physicists is currently on indefinite hold and is likely to remain so. As a result, BEPC will continue to be the facility for this energy region for the foreseeable future.

4.2.3 CESR Luminosity Upgrade

The phased upgrade of CESR to peak luminosities of 10^{33} cm^{-2} s^{-1} is making good progress. Operation with ±2 mrad horizontal crossing angle for the two beams is now routine with beam-beam tune shifts of 0.036 compared with 0.042 for the best head-on operation. Peak luminosities of 2.5×10^{32} cm^{-2} s^{-1} are common at the start of collisions and improving steadily as unwanted multipoles from field errors in special magnets are corrected. With head-on collisions, the best peak luminosity was 3×10^{32} cm^{-2} s^{-1}. Installation of large-aperture final-focus quadrupoles and beam tubes along with the new silicon strip vertex detector in CLEO in early 1995 will make operation much easier and allow for bunch train operation with low backgrounds. Initial test runs with two bunches per train (position of original single bunch) spaced by 28 ns yielded peak luminosities of 2.4×10^{32} cm^{-2} s^{-1} with acceptable detector backgrounds. The total beam current in these tests was comparable to the normal operating currents. For the last month of $\Upsilon(4S)$ running in 1994, two bunches per train was the normal operating mode and the monthly integrated luminosity was the second highest recorded at CESR.

The key to the success of the upgrade plan is the lowering of the higher-order mode impedance of the ring. An initial beam test in CESR in August 1994 of a 500 MHz single cell superconducting rf cavity with all higher-order modes well damped went well. The cavity delivered 155 kW of power to the beam and achieved an accelerating gradient of 6 MV/m. A current of 220 mA was stored with the cavity powering the beam in conjunction with the conventional rf system. By operating CESR at 4.5 GeV the single cell cavity was able to store beam with the conventional rf system detuned. Operation of superconducting cavities in the harsh environment of a high-current storage ring should be similar to that of conventional cavities on the basis of this very successful test.

The elements of the upgrade appear to be in hand, and what remains to be achieved is successful integration of these elements into a smoothly working system. A peak luminosity of 10^{33} cm^{-2} s^{-1} by 1998 seems possible.

4.2.4 B Factories

The luminosity frontier will be the main thrust of these new colliders operating with a center-of-mass energy at the $\Upsilon(4S)$. The goal is to produce as many B mesons as possible in the clean environment of an e^+e^- collider. These colliders have the added advantage of operating with asymmetric beam energies to boost the B's from the $\Upsilon(4S)$ decay so that the time dependence of the B decays can be determined to study CP violation. The clean environment will enable very sensitive tests of rare B decays. The two projects represent the future of circular colliders and promise a rich physics return.

PEP II at SLAC in the US is well underway with completion of the machine scheduled for fall 1998. The Japanese project at KEK, KEK B, is receiving significant funding this fiscal year with an agreed upon plan that calls for commissioning of the storage rings in late 1998. Both machines use as much of existing infrastructure as possible to minimize the cost of the facilities. Because of the large currents and large numbers of bunches, both designs work hard to minimize the higher order mode impedance of the beam environment and feature state of the art feedback systems. A short summary of the main machine parameters is given in Table 13. For details, the reader is referred to the latest versions of the design reports. Achieving these parameters will be a challenge.

Table 13: Selected PEP II and KEK B Parameters.

	PEP II		KEK B	
Parameter	e^+	e^-	e^+	e^-
Beam energy (GeV)	3.1	9.0	3.5	8
Circumference (m)	2199		3016	
Current (A)	2.14	1.48	2.6	1.1
No. bunches	1658	1658	5120	5120
Bunch length (cm)	1.0	1.0	0.32	0.4
β_V/β_H (IP, cm)	$\frac{1.5}{37.5}$	$\frac{3.0}{75}$	$\frac{1.0}{33.0}$	$\frac{1.0}{33.0}$
Crossing angle (mrad)	0		± 10	
Beam-beam tune shift	0.03	0.03	0.05	0.05
Luminosity (10^{33} cm^{-2} s^{-1})	3.0	10.0		

4.2.5 LEP 200

Adding 192 superconducting cavities to LEP to achieve a center-of-mass energy above the W^+W^- threshold will approach the upper limit of what is sensible for the maximum energy of a circular collider using electrons and positrons. Above this energy, the trade off between circumference and total length and voltage gain of the rf system forces a very large cost for the storage ring. Linear colliders are the sensible approach above LEP 2 energies.

The present plan for installation of the superconducting cavities in LEP calls for operation at energies above the W^+W^- threshold in 1996. Because the cross section for W pair production is significantly smaller than the cross section at the Z, a luminosity upgrade is also planned. This will make use of pretzel orbits to increase the number of bunches from 4 to 8. The integrated luminosity goal is to accumulate 500 pb^{-1} (1 pb^{-1} = operation of the collider at a luminosity of 10^{32} cm^{-2} sec^{-1} for 10^4 seconds) by the end of 1999. A short summary of the main machine parameters is given in Table 14. The latest accelerator conference reports should be consulted for details.

5 Advanced Accelerators

Cost played a pivotal role in the demise of the SSC and is a major issue in the LHC. Its importance will increase in the future. As the energy scale of the phenomena being studied rises, it is more than likely that the luminosities needed for precision measurements will rise as well. No technical schemes for producing energies and luminosities much beyond LHC and NHC are in hand. Thus we are being challenged both economically and technically to find acceptable vehicles for carrying us to the multi-TeV energy and precision measurement frontiers.

Table 14: Summary of machine parameters for LEP 200.

Luminosity	7×10^{31} cm^{-2} s^{-1}
Circumference	26.7 km
Bend radius	3.28 km
Maximum beam energy	90 GeV
Superconducting rf cavities	192
Radio frequency voltage	1900 MV
Radio frequency power	15.6 MW
Bunches	8
Bunch current	1 mA

Confronted with this situation in which clear directions have not emerged, it behooves us to proceed on as broad a front as possible in seeking solutions for both accelerator and detector systems at the next frontiers. In carrying out such a program there are three principal directions in which to go. First there is the approach that has served us well for almost half a century: development of improvements to proton synchrotrons and microwave electron linear accelerators. Next on the list is the introduction of completely new systems for acceleration such as those employing lasers, high-current relativistic beams, etc., in which one harnesses technical components that are available from collateral fields or must be especially developed for the purpose. The third approach which has also received attention of late is to consider the collisions of different particles, for which the physics goals and design constraints can be different. Muon and gamma-gamma collisions have been suggested as possible niche accelerators for different purposes and are under continuing investigation.

As we take stock of the current situation and try to lay out strategies that will take us to the frontiers beyond LHC and NHC, we need to keep in mind that our challenge involves a system which must meet cost and many technical requirements simultaneously. What this tells us is that proceeding along any new avenues needs to be disciplined by system studies, including the detectors, from early on. In this way the strengths and weaknesses of potential approaches, including operating and capital cost dimensions, can be confronted and used to guide the evolving R&D.

5.1 Improvements In Conventional Acceleration

5.1.1 Introduction

A natural approach to an advanced accelerator is to scale down the dimensions and rf wavelength (λ) of a conventional structure. This could be a good idea for

several reasons. First, at fixed peak power per unit length (p) or fixed rf pulse energy (u) there is a gain [15] in accelerating gradient (E_a): $E_a \propto p^{1/2}\lambda^{-1/4}$ $E_a \propto u^{1/2}\lambda^{-1}$ Second, the limit imposed by electrical breakdown of the structure walls (E_b) increases [16] : $E_b \propto \lambda^{-1/2}\tau^{1/4} \propto \lambda^{-7/8}$ where τ is the filling time (≤ 1 μs).

Many designs based on scaling linacs to higher frequency are being pursued for the next linear collider; they include collaborations on DLC (DESY Darmstadt), JLC (KEK, Japan) and SLAC–NLC (USA). (The TESLA collaboration is exploring a superconducting structure at lower frequency and gradient [17]).

Two big issues for extending such schemes to the $\geq$ 100 MeV/m level are: 1) developing efficient power sources matched to the structure's requirements on peak power, frequency, and pulse length; and 2) avoiding breakdown/dark current.

5.1.2 Power Sources

There is a world-wide effort on alternative power sources including klystrons, gyroklystrons, EIKs (extended interaction klystrons), TWTs, twystrons, magnicons, gyrotrons, and FELs (free electron lasers) [18]. 11.4 GHz klystrons producing $>$ 50 MW for 0.5 μs with 44% efficiency have already been used to generate 100 MeV/m gradients in an unloaded structure at SLAC [19,20].

Novel concepts such as the cluster klystron [21] and the sheet-beam klystron [22] may significantly improve the overall rf system efficiency by operating at lower beam current densities, thereby permitting the use of highly optimized extraction circuits which should yield high (approaching 60–70%) rf efficiencies. Moreover, in some systems, modulating grids or nonintercepting modulating-anodes (magnicon injection guns) would permit rapid modulating of the klystron beam pulses, thereby permitting the use of DC power supplies and a concomitant increase in modulator efficiency.

5.1.3 Two Beam Accelerators (TBA's)

An alternative power source that might represent a significant simplification is the two-beam accelerator (TBA) concept [23]. In this scheme a high-current (drive) beam runs parallel to the accelerated beam in a separate structure. The drive beam produces radiation via a free electron laser mechanism [Lawrence-Berkeley Laboratory, USA approach] or a relativistic klystron interaction (CLIC, CERN and LBL approach) [24]. This radiation is diverted via output couplers to the high-gradient structure.

The drive beam is periodically re-accelerated (for example, via induction accelerator units or superconducting cavities). This scheme takes advantage of the high peak power and efficiency possible with a relativistic driver (*e.g.*, 1000 MW at 34% efficiency were demonstrated in an FEL at LBL) [25]. The re-acceleration of the drive beam overcomes the need for thousands of separate power sources.

Recent work on TBA's has included extensive modeling of the tolerance on drive beam quality in order to maintain control of rf phase [26], fabrication of scaled high-gradient structures for testing with conventional power sources [27], and development of a new theoretical model that allows comparison of the relativistic klystron and FEL approaches to a TBA [28]. Simulations have shown that an FEL in a standing wave structure enables adequate control of rf phase, if the structure is also designed to suppress BBU instabilities. It has been shown that since the frequency generated by the relativistic klystron interaction is dependent on beam speed rather than energy, the tolerance on energy spread ($\delta\gamma/\gamma$) is relaxed at high γ compared to the FEL interaction [24]. The final choice will depend on how such advantages trade off against the added difficulty of accelerating a bunched drive beam to high γ. Experiments at the CLIC test facility have already reached a 50 MeV/m gradient with a relativistic klystron TBA.

5.2 Advanced Acceleration Methods

5.2.1 Wakefield Accelerators

One step simpler than the TBA's, conceptually at least, are the wakefield accelerator schemes. Here the drive beam excites a wakefield in a structure or a medium (*e.g.*, dielectric or plasma), and the high-energy beam is directly accelerated by this wakefield (*i.e.*, without shunting the wakefield off to a separate structure). In order to overcome a fundamental wakefield theorem [29] and obtain a large transformer ratio (ratio of energy gained per trailing particle to energy per driving particle), various geometries have been proposed. These include noncollinear or hollow drive beams and shaped beams [30] with slowly rising and sharply falling current profiles [31]

Various proof-of-principle experiments were performed in the late 1980's [26,32,33,34]. At Argonne National Laboratory (ANL, USA) Jim Simpson's group used test particles to successfully confirm theoretical predictions of wakefields in hollow dielectric tubes [28] and in plasmas [29]. A multibunch driver experiment at KEK (Japan) led by A. Ogata accelerated trailing particles by 10 MeV over .75 m in a plasma [30]. Currently experiments are planned at ANL and UCLA (USA) to extend the experiments to high-gradients (up to 100 MeV/m) and non-negligible transformer ratio. The early ANL work showed that BBU instability and charging of the walls are critical issues in dielectric tubes.

To overcome these, a design has been developed by which the driving and accelerating beams travel through different tubes. This scheme then resembles the TBAs of the previous section.

5.2.2 Laser Near Field Accelerators

A natural approach to achieving acceleration at laser wavelengths is with miniaturized conventional or unconventional slow-wave structures. Although new micromachining technology using lithographic techniques or open structures may make these feasible to build, some novel approach is still required to make the transverse wakefields (scaling as $1/\gamma^3$) small enough to avoid instabilities and degradation of beam quality. Furthermore, electrical breakdown is obviously an issue. Assuming for the moment that these problems could be overcome, R. Byer has described a scenario for a 1-km-long TeV accelerator with 10^{10} electrons and a rep rate of 120 Hz [35]. To accommodate the beam load and avoid surface damage requires a rectangular slow wave structure 3 cm wide by 1 μ high. The laser needed to fill a 10 cm length of this structure would have a kilowatt of average power. Byer points out that such a laser could be commercially available in four years; and diode pumped solid state lasers already operate with wall plug efficiency of 10%.

5.2.3 Inverse Cerenkov Accelerators

An alternate approach to coupling particles to parallel component of laser electric field is the Inverse Cerenkov Accelerator (ICA). In the ICA the parallel component of E is created by tilting the laser at a slight angle Θ to the particle beam direction in a gaseous medium. By choosing Θ to be the Cerenkov angle ($\Theta = \cos[1/n]$, where n is the refractive index of the gas), the particles remain in phase with the (slowed) laser and can gain energy at a rate $q\vec{v}\vec{E} \approx qcE \sin\Theta_c$. The perpendicular component of E can be nearly canceled (leaving a modest net focusing force) by using an axicon geometry [36]. In a recent experiment led by W. Kimura at Brookhaven National Laboratory (USA) [37], this technique was used to accelerate test particles with a .7 GW CO_2 laser ($\lambda = 10.6$ μ) in an H_2 gas at 2.2 atm ($\Theta = 20$ mrad). Energy gain from 40 MeV to 43.7 MeV over 12 cm was measured for a gradient of 31 MeV/m in agreement with their theoretical model.

Critical issues for this scheme are how to avoid gas ionization by the laser (limiting E), how to maximize n, and hence Θ and $E_\parallel$, without increasing gas pressure and consequent particle beam scattering (*e.g.*, by taking advantage of atomic resonances), and how to stage (by re-focusing the laser beam).

5.2.4 Inverse FEL

There is no limit from breakdown of fields at a focus in a vacuum, but such fields do not accelerate an unperturbed particle. If the particle is bent or wiggled by an external magnetic field, then acceleration is possible.

For fixed field it would be Inverse Synchrotron Acceleration; for a wiggling field it is an Inverse Free Electron Laser (IFEL) [38]. Since, in either case, there need be no structure near the beam, there are no structure induced wakefields; and, since the magnetic fields can be essentially invariant with transverse position, there are no other transverse wake fields. So, unlike most other advanced acceleration schemes, an IFEL is peculiarly suitable for accelerating very small emittances. Unfortunately loss of energy from direct synchrotron radiation sets an effective limit on the maximum energy achievable. For electrons, this limit is at only about 50 GeV [39]; *i.e.*, at an energy already obtained, but for muons the limit would be much higher. An experiment to demonstrate significant IFEL Acceleration is in preparation [40] at the BNL Accelerator Test Facility (ATF) using a CO_2 laser and a pulsed magnetic wiggler.

5.2.5 Plasma Acceleration

Another approach to utilizing the high peak power of lasers is to use them to drive longitudinal space charge waves in a plasma. Plasma waves are accelerating structures that support large parallel electric fields and are immune from electrical breakdown. The plasma waves can be driven resonantly by the radiation pressure of a train of laser pulses [41,42], separated approximately by a plasma period $2\pi/\omega_p$, where $\omega_p = [4\pi\, n_0\, e^2\, /\, m]^{1/2}$ as in the beat wave accelerator or by a single short ($\approx \pi/\omega_p$) pulse as in the laser wakefield accelerator [37,43]. In the beatwave scheme the accelerating gradient scales,

$$E_\parallel = \frac{\sqrt{n_0}}{4} \int_0^\tau \alpha_1\, \alpha_2\, \omega_p\, dt, \qquad (8)$$

where $\omega_{1,2} = eE_{1,2}/m\omega_{1,2}c$ is the normalized oscillatory velocity in the laser field, $\omega_1 - \omega_2 = \omega_p$, n_0 is in cm^{-3} and τ is the smaller of the laser pulse length, the relativistic detuning time ($\approx 7[\alpha_1\alpha_2]^{-2/3}/\omega_p$) and the time scale for ion instabilities (a few times the ion plasma period $\approx 43 \times 2\pi/\omega_p$).

Several groups including C. Joshi *et al.* at UCLA (USA), A. E. Dangor *et al.* at Rutherford (UK), F. Amiranoff *et al.* at Ecole Polytechnique (France) and Y. Kitagawa *et al.* in Osaka (Japan) have performed beat wave experiments in the last decade, successfully demonstrating the generation of plasma waves with longitudinal fields of 1–3 GeV/m and phase velocity [44] $\approx c$. Recently, UCLA [45], Osaka [46], and a group at

the National Research Council (Canada) [47] have also reported acceleration of injected particles.

The UCLA group accelerated $\sim 10^5$ test particles (approximately 1% of the randomly phased injected particles from 2 MeV to up to 30 MeV over 1 cm in a plasma of density 8×10^{15} cm^{-3}. This corresponds to a gradient of 3 GeV/m. The energy gain was limited by the focal depth of their CO_2 lasers. The experiment confirmed earlier simulations and theoretical work predicting that competing instabilities could be avoided by employing short laser pulses (compared to an ion plasma period $\approx 43 \times 2\pi/\omega_p$) of sufficient amplitude ($eE/m\omega c \geq 0.1$). Based on these results, it is possible to extrapolate the UCLA design to a 1 GeV experiment over $\sim$ 10 cm using T-class lasers beating in a 10^{17} cm^{-3} density plasma.

The critical issues for laser-plasma accelerators beyond 1 GeV include diffraction and staging; long time scale instabilities and pump evolution [48], dephasing [49], beam loading; beam quality, and efficiency [50]. Preformed plasma channels have been explored recently both theoretically [51,52], and experimentally [53] as a means of confining the laser for many diffraction lengths as well as for creating accelerating and focusing fields that are optimal for high beam quality.

5.3 Alternative Particles

5.3.1 Linear Colliders with γ–γ Collisions

There exist strong arguments that the particle physics one can study with a linear electron-positron collider is special and complementary to that of a hadron supercollider. Similarly the study of electron-photon and photon-photon collisions would provide unique access to some areas of fundamental physics plus some not unwelcome redundancy with measurements obtained from electron-positron collisions. Physics goals for a gamma-gamma collider are significant indeed, and are presented below.

Initial studies reveal no show-stoppers to γ–γ and e–γ colliders. Therefore, it would be prudent that the conceptual design of a linear collider include multiple interaction regions, one of which is dedicated to e–γ and γ–γ collisions. Given that e^+e^-, e^-–γ, and γ–γ colliders are the same except for the interaction region, the incremental cost of adding gamma collisions to the capabilities at one of the interaction regions is relatively small.

The R&D required for e–γ, and γ–γ colliders, in addition to that for the e^+e^- machine would be:

- detectors and masking;
- high-power lasers, including FEL's;
- special final focus components;
- bright sources of polarized electrons; and
- high-power, low-loss optical components

One initial step, for example, could be a Photon Linear Collider with a center-of-mass energy of 80–180 GeV. This collider will be less expensive than other variants (less energy, positrons are not necessary), but it would have high discovery potential in Higgs physics, etc.

5.3.2 Physics Goals for a γ–γ Collider

The structure functions of the photon, probed by deep inelastic scattering from a photon target, is a fundamental and largely unresolved area of investigation in quantum chromodynamics. Clearly the electron-photon collision option would provide the paramount facility for these studies. In another important area of QCD, photon-photon collisions would allow studies of the top quark threshold region that would complement studies performed in electron-positron collisions. Here some unique measurements are possible using polarized photon beams: large circular polarization will allow direct observation of p-wave toponium, not possible in electron-positron collisions, while with linear polarization it may also be possible to make very sensitive measurements of the strong coupling constant.

Study of W boson pair production in photon-photon collisions provides the most sensitive tests for quartic anomalous interactions of the electroweak gauge bosons. The photon-photon option also provides some unique advantages for Higgs boson studies. The two photon width of a Higgs boson is most directly measured here; it is a fundamental probe both of the electroweak theory and for electrically charged ultraheavy quanta which would affect the two photon rate if their mass is generated by the Higgs boson. The search for supersymmetric Higgs bosons is also enhanced by the photon-photon option. The heavy scalar and pseudoscalar of the minimal supersymmetric model must be produced together in the same event in electron-positron collisions, requiring energy greater than the sum of their masses, but in photon-photon collisions they can be produced and observed individually. The circular polarization of the photon beams is an important asset in these studies, both enhancing the signal and suppressing the background. Linear photon polarization may also be useful, since it would allow direct measurement of the properties of Higgs bosons, which might not be directly measured in any other way.

5.3.3 μ^+–μ^- Colliders

Lepton colliders produce simple interactions essential in the exploration of new particle states. Extension of e^+e^- colliders to multi-TeV energies is performance-constrained by radiation and "beamstrahlung" effects, which increase as $(E_c/m_c)^4$ and cost-constrained by the need for two full-energy linacs [54]. However muons

Table 15: Parameter list for a 4 TeV $\mu^+\mu^-$ Collider.

Parameter	Symbol	Value
Energy/beam	E_μ	2 TeV
Luminosity	$\mathrm{L} = \frac{f_0 n_s n_b N_\mu^2}{4\pi\sigma^2}$	$3\times10^{34}\,\mathrm{cm}^{-2}\,\mathrm{s}^{-1}$
Source Parameters		
Proton energy	E_p	30 GeV
Protons/pulse	N_p	$2\times3\times10^{13}$
Pulse rate	f_0	10 Hz
μ-production acceptance	μ/p	0.15
μ-survival allowance	$N_\mu/N_{\mathrm{source}}$	0.33
Collider Parameters		
Number of μ/bunch	$N_{\Delta\pm}$	1.5×10^{12}
Number of bunches	$4n_B$	1
Luminosity turns	n_s	900
Normalized emittance	ϵ_N	3×10^{-5} m-rad
μ-beam emittance	$\epsilon_t = \epsilon_N/\gamma$	1.5×10^{-9} m-rad
Interaction focus	β^*	0.3 cm
Beam size at IP	$\sigma = \sqrt{\epsilon_t}\,\beta_0$	2.1 μm

(heavy electrons with $m_\mu = 200\ \mathrm{m}_e$) have negligible beamstrahlung and can be accelerated and stored in rings. The liabilities of muons are that they decay, with a lifetime of $2.2\times10^{-6}\ E_\mu/m_\mu$ s, and that they are created through decay into a diffuse phase space. But a study [55] suggests that a $\mu^+\mu^-$ collider, with an energy of $E_{\mathrm{cm}} = 2E_\mu = 4$ TeV, and luminosity of $L = 3\times10^{34}\,\mathrm{cm}^{-2}\,\mathrm{s}^{-1}$, might be possible using only existing technical capabilities.

The possibility of muon ($\mu^+\mu^-$) colliders has been introduced by Skrinsky *et al.*, [56] and Neuffer [57]. More recently, several mini-workshops have greatly increased the level of discussion [51,58,59,60]. Palmer and Neuffer [51] have introduced improvements, and developed a complete scenario. Table 15 shows their parameters. The design consists of a muon source, a muon collection, cooling and compression system, a recirculating linac system for acceleration, and a full-energy collider with detectors for multiturn high-luminosity collisions.

The μ-source driver is a high-intensity rapid-cycling (10 Hz) synchrotron, similar in scope to the proposed 30 GeV facility, KAON [61]. Two bunches of 3×10^{18} protons each are accelerated and extracted into separate lines for μ^+ and μ^- production. (Separate lines permit use of higher-acceptance $\pi\rightarrow\mu$ capture lines.) Each bunch collides into a target, producing π's ($\sim 1\pi$/interacting p) over a broad energy and angular range. The target is followed by Li lenses which collect the πs into a large-aperture, strong-focusing transport line, which has a large energy width and angular acceptance. This line is sufficiently long to insure $\pi\rightarrow\mu$ decay, plus bunch lengthening. Bunch lengthening is followed by a nonlinear rf acceleration system which implements an rf rotation, in which the bunch is lengthened while the energy spread decreases. The μ beam is then matched into a beam cooling system. From Monte Carlo simulations, they obtain ~ 0.2 captured μs per initial proton.

For collider intensities, the phase-space volume must be reduced. This is obtained by "ionization cooling" of muons which is described in detail in references [52,53,62]. In ionization cooling, beam transverse and longitudinal energy losses in passing through a material medium are followed by coherent reacceleration, resulting in beam phase-space reduction [63]. The coherent cooling is opposed by the randomizing (heating) effects of multiple scattering and energy straggling. To minimize energy straggling, cooling is done at low relativistic energies ($E_\mu \sim 300$ MeV), in a strong-focusing lens which maintains small beam size over extended lengths, and a low-Z material. A series of about 20 Li current-carrying rods, where the high current provides strong radial focusing, alternating with linear accelerators provide adequate transverse cooling.

Phase-space exchange in wedge absorbers is used to balance the longitudinal and transverse cooling to design parameters. In this scenario, they cool only with ionization cooling in conducting rods, and that is sufficient. However, other techniques, such as ionization cooling in focusing transports or rings, or optical stochastic cooling [64], may permit improvements.

Following cooling and preacceleration, the beams are accelerated to full energy (2 TeV). A full-energy linac would work, but it would be expensive and does not use our ability to recirculate μ's. A recirculating linac similar to CEBAF [65] could obtain acceleration to full energy in 10–20 recirculations, using only 200–100 GeV of linac. After acceleration, the μ^+ and μ^- bunches would be injected into the 2-TeV superconducting storage ring (~ 1 km radius), with collisions in two interaction areas. The beam size at collision is focused to $\sigma \approx 2\ \mu$m, similar to hadron collider values. For a mean bending field of 6 T the bunches circulate for ~ 900 turns before decay.

The greatest uncertainty in such a concept is whether the detector background can be made acceptable. Electrons, from decay of muons in the storage ring, collide with the walls and collimators yielding massive electromagnetic showers, hadronic particles and significant numbers of lower energy muons. If this problem can be solved, the $\mu^+\mu^-$ collider may well provide the only economically and technically feasible access to energies beyond the LHC.

6 Conclusions

The Accelerator Physics, Technologies, and Facilities Working Group has, over the course of this study, come to several conclusions with regard to the need for continuing support of accelerator-directed research and development in the United States. It is evident from past experience that research into accelerator technologies is required for the long-term health of the field of high-energy physics. Our conclusions in this regard are most easily grouped into three categories: hadron colliders, electron linear colliders, and novel technologies.

For high-energy hadron colliders, superconducting magnets are the enabling technology. As such, reassembly of a United States superconducting magnet research and development program is critical to the future. The key to increasing the luminosity of the Tevatron proton-antiproton collider has been, and will continue to be, increasing the antiproton production rate. Development of this capability deserves continuing support. Significant participation in the Large Hadron Collider project is expected to be a valuable and important component of a United States program for hadron collider research and development. Such participation would be most valuable if targeted toward those areas that represent the greatest challenges in moving toward the future; for example, superconducting magnet and beam-tube vacuum technologies. Finally, there are new ideas for overall systems designs for a 60 TeV collider facility that could be constructed sometime following completion of the LHC. These ideas deserve to be pursued.

For electron linear colliders, the enabling technologies are the high-gradient acceleration system: radio frequency power sources, accelerator structures, etc. The technology required to support a next-generation linear collider has made significant advances over the past several years, and is expected to reach maturity during the next few years. There are linear collider test facilities now under construction that should be completed as expeditiously as possible. Finally, conceptual designs of next-generation linear colliders based on proven technologies should be developed over the next two to three years.

To conclude, we expect that new novel technologies and/or different types of collider may be required to allow high-energy physicists to explore the multi–TeV scale (a muon collider is a possible example). Continued investment in generic accelerator research is required if we are to continue to open new experimental opportunities at an ever expanding energy frontier.

Acknowledgments

The conveners wish to express their gratitude to the Working Group members for their contributions, and to the conveners of the other working groups for their useful suggestions and comments. We also appreciate the work of participatants of the Indiana Workshop on Future Hadron Facilities for input into Section 2.

References

[1] Proc. Workshop on Future Hadron Facilities in the US, Bloomington, Indiana, 1994; Fermilab–TM–1907.

[2] SSC Central Design Group, "Conceptual Design of the Superconducting Super Collider," SSC–SR–2020 (1986).

[3] A. Piwinski, Proc. 9th Int. Conf. High Energy Part. Accel., **405** (1974).

[4] Convener's Note: Following the workshop, a promising concept '(multibatch coalescing) has been proposed for the Main Injector. If viable, this would reduce the need for new accelerators to one.

[5] Contributed by N. Phinney.

[6] Contributed by R. Siemann; see also 8/94 Linac Conf. paper, SLAC–PUB–6646 (1994).

[7] Contributed by K. Takata

[8] Contributed by I. Wilson, CERN/SL 94–89 (RF) CLIC Note 253.

[9] Contributed by R. Brinkmann, N. Holtkamp, and T. Weiland.

[10] The TESLA Collaboration: CERN, Cornell, CE–S DAPHNIA, DESY, Fermilab, Gesamthochschule Wuppertal, IHEP Beijing, INFN Frascati, LASA Milan, IPN Orsay, Johan-W. Goethe U. Frankfurt, KFK Karlsruhe, LAL Orsay, SEFT Helsinki, TH Darmstadt, TU Berlin, TU Dresden, UCLA Los Angeles.

[11] Contributed by M. Tigner for the TESLA Collaboration (Ref. [10]); see also H. T. Edwards, " TESLA Parameters Update, a Progress Report to be published in Part. Accel. by Gordon and Breach.

[12] Contributed by P. K. Tannebaum for the FFTB Collaboration (Ref. [13]); see also V. Balakin *et al.*, *Phys. Rev. Lett.* **74**, No. **13**, 2479 (1974).

[13] The FFTB Collaboration: Deutsches Elektronen–Synchrotron, DESY, Hamburg, Germany; Fermi National Laboratory, Batavia, IL, USA; The Budker Institute for Nuclear Physics, Russia; Laboratoire de l'Accelerateur Lineaire, Orsay, France; Max–Planck–Institute, Munich, Germany; National Laboratory for High Energy Physics, KEK, Tsukuba, Japan; and Stanford Linear Accelerator Center, Stanford University, tanford,CA, USA.

[14] Contributed by R. Ruth; see also R. D. Ruth *et al.*, "The Next Linear Collider Test Accelerator," Proc. PAC93, Washington, DC., and in SLAC–PUB–6252.

[15] P. Wilson, "Pulsed RF Technology for Future Linear Colliders," invited talk at the April 21, 1992 APS meeting in Washington DC.

[16] P. Wilson, private communication.

[17] R.H. Siemann, in Proc. 1993 Part. Accel. Conf., Washington DC, (IEEE, Piscataway, NJ, 1993) p. 532.

[18] V. Granatstein and C. Striffler, Proc. Advanced Accelerator Concepts, Port Jefferson, NY, 1992, AIP Conf. Proc. **279**, ed. J. Wurtele (AIP, NY, 1993) p. 1.

[19] T. Lavine, private communication; and R. Ruth *et al.*, Ref. [8], p. 543.

[20] "NLC Test Accelerator, Conceptual Design Report,"
SLAC Report–411, August 1993 (available from National Technical Information Service, US Dept. of Commerce, 5285 Port Royal Road., Springfield, VA 22161).

[21] R.B. Palmer, W.B. Herrmannsfeldt, K.R. Eppley, "An Immersed Field Cluster Klystron," Proc. Int. Conf. High Energy Accel., Tsukuba, Japan, 1989; and SLAC–PUB–5026 (1989).

[22] D.U.L. Yu, J.S. Kim, and P.B. Wilson, "Design of a High-Power Sheet-Beam Klystron," Proc. Advanced Accelerator Concepts, op. cit., p. 85–102.

[23] A.M. Sessler in Laser Acceleration of Particles, ed. P.J. Channell (AIP, NY, 1982) p. 154; A.M. Sessler, D.H. Whittum, W. M. Sharp, M.A. Makowski, and J.S. Wurtele, *Nucl. Inst. and Meth.* A **306**, 592 (1991).

[24] S. Van der Meer, *Part. Accel.* **30**, 127 (1990); W. Schnell, Proc. ICFA Workshop on e^+e^- Linear Colliders, ICFA 93–154, ed. R. Settles, 1993, p. 267; CLIC Study Group Report in Ref. [3], p. 540.

[25] T. Orzechowski *et al., Phys. Rev. Lett.* **57**, 2172 (1986).

[26] W.M. Sharp *et al.*, in Proc. Intense Microwave and Part. Beams II, O/E Lase 91, Los Angeles, in Proc. Int. Soc. OptEng. (SPIE) (1991).

[27] T. Lavine, private communication.

[28] J.S. Wurtele *et al.*, in Ref. [4], p. 143.

[29] S. Heifets and S. Kheifets, *Rev. Mod. Phys.* **63**, 631 (1991).

[30] W. Bialowons *et al.*, in New Developments in Part. Accel. Techniques, Orsay, France, ed. S. Turner, (CERN 87–11, Geneva, 1987) p. 298.

[31] K.L.F. Bane, P. Chen, and P.B. Wilson, *IEEE Trans. Nucl. Sci.* **32**, 3524 (1985).

[32] W. Gai *et al., Phys. Rev. Lett.* **61**, 24 (1988).

[33] J. B. Rosenzweig *et al., Phys. Rev. Lett.* **61**, 98 (1988).

[34] A. Ogata *et al.*, in Proc. HEACC 89, Tsukuba, Japan.

[35] R. Byer, in Proc. Adv. Accel. Concepts. Workshop, Lake Geneva, WI, 1994.

[36] G. Fontana and R. Pantell, *J. Appl. Phys.* **54**, 4285 (1983).

[37] W. Kimura, in Proc. Adv. Accel. Concepts. Workshop, Lake Geneva, WI, 1994.

[38] R.B. Palmer, *J. Appl. Phys.* **43**, 3014, 1972.

[39] C. Pellegrini, P. Sprangle, and W. Zakowicz, Int. Conf. on High Energy Accelerators, 1983.

[40] IFEL Exp. at BNL

[41] T. Tajima and J.M. Dawson, *Phys. Rev. Lett.* **43**, 267 (1979).

[42] Vi Berezhiani and Ig. Murusidze, *Physica Scripta* **45**, 87 (1992); D. Umstadter *et al., Phys. Rev. Lett.* **72**, 1224 (1994).

[43] P. Sprangle *et al., Appl. Phys. Lett.* **53**, 2146 (1988).

[44] C.E. Clayton *et al., Phys. Rev. Lett.* **55**, 1962 (1985); A.E. Dangor *et al., Physica Scripta* T **30**, 107 (1990); Y. Kitagawa *et al., Phys. Rev. Lett.* **68**, 45 (1992); F. Amiranoff *et al., Phys. Rev. Lett.* **68**, 4780 (1992).

[45] M. Everett *et al., Nature* **368**, 527 (1994).

[46] A. Ogata, private communication.

[47] N. Ebrahim, private communication.

[48] T. Antonsen and P. Mora, *Phys. Rev. Lett.* **69**, 2204 (1992); P. Sprangle *et al.*, **69**, 2200 (1992); W. B. Mori *et al., Phys. Rev. Lett.* **72**, 1482 (1994); J.S. Wurtele and G. Shvets, submitted to *Phys. Rev. Lett.* (1993); P. Gibbon and A.R. Bell, *Phys. Rev. Lett.* **61**, 1599 (1988). These works examine long time scale instabilities that may be both deleterious and beneficial. Recent simulations have shown that forward Raman scatter, or self-modulations of a single frequency laser, can be used to accelerate large numbers of self-trapped plasma electrons to order 100 MeV in a millimeter. Such an accelerator could be an economical tool for applications that do not require high beam quality.

[49] T. Katsouleas and J.M. Dawson, *Phys. Rev. Lett.* **51**, 392 (1983).

[50] T. Katsouleas *et al., Part. Accel. Conf. Proc.* , 81 (1987).

[51] T. Krall *et al., Phys. Rev.* E **48**, 2157 (1993).

[52] T. Katsouleas *et al.*, Ref. (14), p. 480.

[53] G. Durfee and H. Milchberg, *Phys. Rev. Lett.* **71**, 2409 (1993).

[54] M. Tigner, Ref. [14], p. 1.

[55] R.B. Palmer, David Neuffer, and J. Gallardo, Proc. Advanced Accelerator Concepts, Lake Geneva, WI, 1994.

[56] E.A. Perevedentsev and A.N. Skrinsky, Proc. 12th Int. Conf. on High Energy Accel., 485 (1983); A.N. Skrinsky and V.V. Parkhomchuk, *Sov. J. Nucl. Physics* **12**, 3 (1981).

[57] D. Neuffer, *Part. Accel.*, **14**, 75 (1983); Proc. 12th Int. Conf on High Energy Accel., **481**, 1983); Advanced Accelerator Concepts, AIP Conf. Proc. **156**, 201 (1987).

[58] R.J. Noble, in Ref. (14), p. 949.

[59] Proc. Muon Collider Workshop, Los Alamos National Laboratory Report LA–UR–93–866, ed. H.A. Thiessen, 1993.

[60] Proc. Mini-Workshop on $\mu^+\mu^-$ Colliders; Particle Physics and Design, Napa CA, 1994, ed. D. Cline, to be published in *Nucl. Instand Meth.*

[61] *KAON Factory proposal, TRIUMF*, KAON internal report (Vancouver, Canada, 1990).

[62] D. Neuffer, to be published in *Nucl. Inst. and Methods* (1994).

[63] Ionization cooling is not practical for protons and electrons because of nuclear scattering (ps) and bremstrahlung (*e*s) effects, but is for μs, and the necessary energy losses are easily obtained within the μ lifetime.

[64] A.A. Mikhailichenko and M.S. Zolotorev, *Phys. Rev. Lett.* **71**, 4146 (1993).

[65] CEBAF Design Report, CEBAF internal report (CEBAF, Newport News, VA, 1986).